NITRIDES OF METALS OF THE FIRST TRANSITION SERIES

R. Juza

Institut für anorganische Chemie der Universität Kiel, Kiel, Germany

I. Introduction

Transition metal nitrides have been widely studied recently. From the original and somewhat generalized concept of metallic intercalation compounds, several different types have now emerged, which often have quite different characteristics. Titanium nitride, for example, is a substance with the electrical conductivity of a good metallic conductor and the hardness of diamond. Regular and at the same time big changes in the properties of nitrides occur with increasing atomic number in the transition metal series, and there are also marked crystallographic regularities. The nitrides of chromium, manganese, and iron are also of theoretical interest because of the incidence of ferromagnetism, antiferromagnetism, and ferrimagnetism.

Quite a new concept of the bonding in these substances has also emerged as a result of improvements in older techniques, such as X-ray crystallography and magnetic measurements, and the introduction of new methods, such as neutron diffraction, for the elucidation of magnetic structures. Interpretation of the results of these studies has been greatly helped by further developments in theories of the chemical bond, particularly the Valence Bond and Molecular Orbital theories, and also by applications of the theory of metallic bonding. The study of nitrides has also been greatly stimulated by technical developments. Applications will not in general be discussed in this article, although those which have stimulated scientific research will be referred to briefly.

Nitrides of metals of the fourth and fifth groups have long been of importance in high-melting cermets, as have some of the carbides. In

combination with a metal such as cobalt they have found widespread use as hard-cast alloys. Fashioning is done by the methods of powder metallurgy, involving sintering and hot-pressing at high temperatures. Their notably high melting points and relatively good nonscaling properties have made these materials of interest in connection with problems of jet propulsion and rocket technology. In addition to the preparation of sintered products, the production of thin coatings on metallic or ceramic base materials is also important. The high melting points, coupled with the possibility of fashioning by the methods of powder metallurgy, have also resulted in the manufacture of refractory vessels for metallurgical work which can be used in melting alloys of the b-group metals. In this connection the use of ternary compounds which contain metal from the b-groups as well as a transition metal may be noted. The chemical resistance and high electrical conductivity lead to applications as electrode materials in fused salt electrolysis. The compounds are also interesting as superconductors because of their relatively high transition temperatures.

Study of the nitrides of metals in Groups 6–8, especially double nitrides and carbidenitrides of these metals, has been stimulated by *inter alia* the steel industry. Such phases play a key role in nitrided steels, although they occur independently of the process of hardening by nitriding.

II. Binary Compounds

A. Phases

Before discussing the chemical and physical properties of these compounds their constitutions will be dealt with. If they were ionic the formulas would be a sufficient indication. It is also necessary in this case to specify, where possible, stability ranges and, as far as is known, the dependence of these on temperature. The crystal structure is also required as a means of characterizing a particular compound.

1. Survey of Interstitial Structures

G. Hägg recognized that there is a common structural principle for the metallic nitrides (*51*). The structure is determined by the metal atoms, which are substantially bigger than the nitrogen atom. In the vast majority of compounds the metal atoms are arranged in either cubic or hexagonal close packing. Nitrogen atoms are intercalated in the octahedral holes in the metal structure and this is the origin of the terms "intercalation compound" and "intercalation phase" introduced by Hägg.

In the close-packed cubic unit cell (Fig. 1) there are four octahedral holes situated in the center of the cell and in the middle of the edges. The octahedron of metal atoms associated with the nitrogen in the $\frac{1}{2}\frac{1}{2}\frac{1}{2}$ position

is illustrated. A simple geometrical relationship shows that the nitrogen atoms just fit into these holes when the radii of nitrogen and metal are in the ratio $r_N : r_{Me} = 0.41$. If the nonmetal does not fill the holes, which is so in the case of metallic hydrides, it goes into the smaller tetrahedral holes. If the nonmetal is somewhat too large the metal atom lattice is expanded and metal-metal contact is lost. Expansion of the metal lattice is observed up

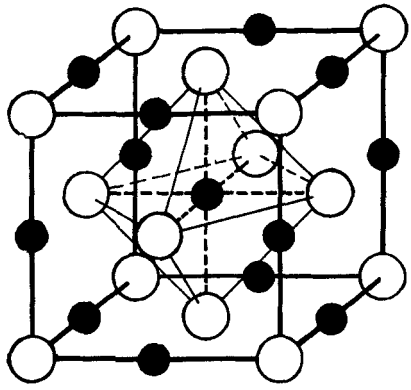

FIG. 1. Lattice of nitrides of the type MeN (NaCl type): ○ Me; • N.

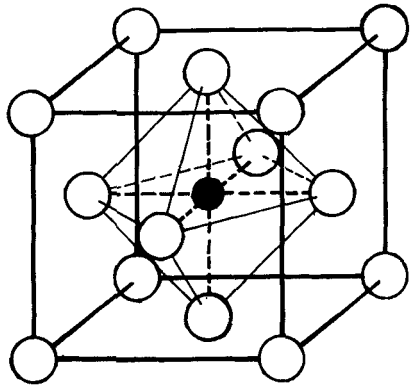

FIG. 2. Lattice of nitrides of the type Me_4N (perovskite type): ○ Me; • N.

to the value $r_N : r_{Me} = 0.59$. If this value is exceeded, as for example in Fe_3C, more complex structures result.

Two types of compound may be derived from the cubic close-packed arrangement. If all octahedral holes in the cubic face-centered metal atom lattice are occupied, the composition is MeN (type B1, *sodium chloride lattice*). A substantial percentage of the positions in the nitrogen sublattice may remain unoccupied when, as is generally the case, the metal lattice is fully populated. The vacancies are then distributed statistically and one

again speaks of a "NaCl lattice," although the composition may deviate very appreciably from MeN.

If only the $\frac{1}{2}\frac{1}{2}\frac{1}{2}$ position in the face-centered cubic unit cell is occupied by nitrogen (Fig. 2), the composition becomes Me_4N. Only one quarter of the available octahedral holes are then occupied. This occurs in such a way that only one of two neighboring octahedral holes contains nitrogen. The four metal atoms are no longer equivalent with respect to nitrogen, the atom in the 000 position being more distant. This is reflected in the properties of the nitrides: they are now called "*perovskite*-type nitrides." Their analogy to perovskite is expressed by the formula $Me_cN(Me_f)_3$ (type L'10), where Me_c is the atom at the corner of the cube and Me_f represents the three in the middle of the faces.

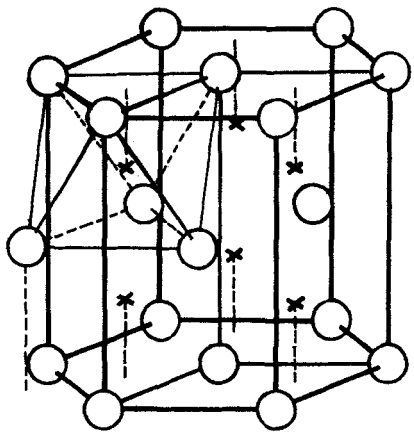

FIG. 3. Hexagonal close packing of metal atoms in the nitrides Me_3N to $\sim Me_2N$: ○ Me; × octahedral holes.

The framework for nitrides which crystallize in the hexagonal system is provided by metal atoms with a *hexagonal close-packed* arrangement, compositions varying in the first transition series between Me_3N and Me_2N. The triple hexagonal close-packed unit cell shown in Fig. 3 contains six octahedral holes for six metal atoms: these are indicated in the figure by crosses. One octahedron formed by the six neighboring metal atoms is shown. It includes one metal atom from the neighboring cell. Octahedral holes are, however, filled by nitrogen to the extent of only 33–50%, corresponding with the formulas Me_3N and Me_2N. When nitrogen is distributed statistically the unit cell of the nitride is the same as that for the hexagonal close-packed metal lattice. With ordered arrangements of nitrogen, superstructures occur, which will be discussed for the hexagonal iron nitrides (cf. Section II,A,2*f*).

2. Nitrides of the Metals

Table I summarizes the phases, their compositions, and structural data. Where the phase limits are known they are given with their lattice constants, measured at room temperature and shown by a cross. It is difficult to avoid a certain measure of inconsistency in writing the formulas.

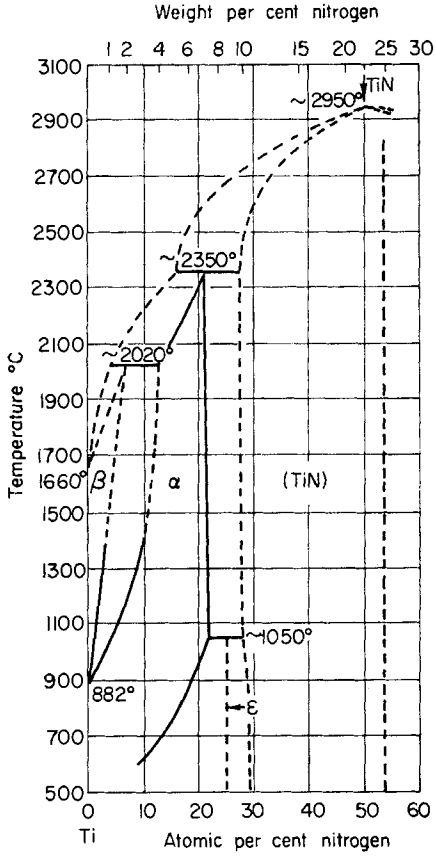

FIG. 4. The titanium/nitrogen system (*55*).

a. Scandium. The only compound of *scandium* to exist is ScN, which crystallizes with an NaCl lattice and is thus in line with the MeN phases of subsequent elements. Unlike them, however, scandium nitride has a stoichiometric composition (*8*) or a very narrow stability range (*147*).

b. Titanium. The system *titanium*/nitrogen (cf. Fig. 4) (*55*) is typical of intercalated structures in the sense of Hägg's formulation (*50, 51*). Hexagonal close-packed α-titanium takes up nitrogen in solid solution

TABLE I
STRUCTURAL DATA

Phase	Structural type and space group	Composition[a]	Lattice constants (Å)			Reference	Additional readings
			a	*b*	*c*		
ScN	B1, O_h^5	ScN	4.45	—	—	(*8*)	—
		$ScN_{0.970}$	4.499	—	—	(*147*)	—
δ-TiN	B1, O_h^5	$Ti_{0.875}N$	4.21	—	—	(*14*)	(*14, 60, 117, 131*)
		x $TiN_{1.00}$	4.234	—	—	(*28*)	—
		x $TiN_{0.42}$	4.215	—	—	(*28*)	—
ε-Ti_2N	Tetragonal, D_{4h}^{14}	$TiN_{0.50}$	4.945	—	3.034	(*60*)	(*127*)
γ-VN	B1, O_h^5	$VN_{1.00}$	4.126	—	—	(*53*)	(*15, 33*)
		$VN_{0.71}$	4.064	—	—	(*53*)	—
β-V_3N	L'3, D_{6h}^4	x $VN_{0.43}$	2.835	—	4.541	(*53*)	—
		x $VN_{0.37}$	2.831	—	4.533	(*53*)	—
γ-CrN	B1, O_h^5	$CrN_{1.0}$	4.140	—	—	(*11*)	(*34, 135*)
CrN antif.	Orthorhombic, D_{2h}^{16}	$CrN_{1.0}$	5.757	2.964	4.134	(*26*)	—
β-Cr_2N	L'3, D_{6h}^4	x $Cr_2N_{1.0}$	2.768	—	4.469	(*34*)	(*137*)
		x $Cr_2N_{0.75}$	2.742	—	4.429	(*34*)	—
MnN ?	Cubic ?	$MnN_{1.04}$	4.435	—	—	(*126*)	—
ϑ-Mn_6N_5	Tetragonal face-centered	x $Mn_6N_{5.25}$	4.2218	—	4.1136	(*107*)	—
		x Mn_6N_5	4.2145	—	4.1486	(*107*)	—
η-Mn_3N_2	L'6, D_{4h}^{17}	x $Mn_3N_{2.08}$	4.2074	—	4.0410	(*107*)	(*49, 126*)
		x $Mn_3N_{1.85}$	4.2044	—	4.0464	(*107*)	—

ζ-Mn_2N	L'3, D_{6h}^4	x	$Mn_2N_{1.06}$	2.8179	—	4.5346	(*107*)	(*19, 49, 50*)
		x	$Mn_2N_{0.79}$	2.7757	—	4.5284	(*107*)	—
ϵ-Mn_4N	L'1, O_h^5	x	Mn_4N	3.863	—	—	(*87*)	(*18, 49*)
		x	$Mn_4N_{0.435}$	3.763	—	—	(*87*)	—
δ-Mn_xN	Tetragonal		$Mn_{9.2}N$	3.764	—	3.729	(*87*)	—
	face-centered		$Mn_{25.3}N$	3.765	—	3.610	(*87*)	—
ζ-Fe_2N	Orthorhombic		$Fe_2N_{1.0}$	5.512	4.820	4.416	(*72*)	(*17, 20, 21*)
ϵ-Fe_2N	L'3, D_{6h}^4	x	$Fe_2N_{1.0}$	2.77	—	4.42	(*48*)	—
ϵ-Fe_3N	L'3, D_{6h}^4	x	$Fe_3N_{1.0}$	2.695	—	4.362	(*48*)	—
	L'3, D_3^1		Fe_2N	$2.765 \times \sqrt{3}$	—	4.41	(*136*)	(*20, 21*)
	D_3^1		$Fe_{24}N_{10}$	$2.764 \times 2\sqrt{3}$	—	4.420	(*67*)	—
γ'-Fe_4N	O_h^5	x	$Fe_3N_{1.1}$	3.793	—	—	(*132*)	(*48, 67, 136, 176*)
		x	$Fe_4N_{0.89}$	3.783	—	—	(*132*)	—
α''-Fe_8N	L'6, D_{4h}^{17}		$Fe_8N_{1.0}$	5.72	—	6.29	(*71*)	(*52, 69*)
CoN	Cubic (blende)		CoN	4.28	—	—	(*78*)	—
	Cubic (NaCl type)		—	4.27	—	—	(*154*)	—
Co_2N	Orthorhombic, D_{2h}^{12}		$Co_2N_{1.0}$	2.848	4.636	4.339	(*89*)	(*25*)
Co_3N	L'3, hexagonal		$Co_3N_{1.06}$	$2.663 \times \sqrt{3}$	—	4.360	(*89*)	(*170*)
Co_4N	L'1, O_h^5		$Co_4N_{1.0}$	3.738	—	—	(*170*)	—
Ni_3N	L'3, hexagonal		$Ni_3N_{1.0}$	$2.670 \times \sqrt{3}$	—	4.307	(*90*)	(*69*)
Ni_4N	L'1, O_h^5		$Ni_4N_{1.0}$	3.72	—	—	(*169*)	(*9*)
Cu_3N	$D0_9$, O_h^1		$Cu_3N_{1.0}$	3.807	—	—	(*82*)	—

[a] Symbol x indicates lattice constants of the specimen at the phase boundaries.

and thus forms an "intercalated mixed crystal." Because of this intercalation, the hexagonal close-packed arrangement of the metal, which is transformed into a cubic body-centered arrangement at 882°C for the pure metal, is stabilized at higher temperatures, probably to about 2350°C. Nitrogen is situated in the octahedral holes of the hexagonal close-packed titanium lattice (cf. Fig. 3).

The solubility of nitrogen in body-centered cubic β-titanium, which is stable above 882°C, is substantially lower. Only highly distorted "octahedral holes" are available in this type of structure, and the relatively complicated process of intercalation of a nonmetal in such holes has been studied only for the system iron-nitrogen (Section II,A,2).

Apart from these two solid solutions, the diagram is dominated by the δ-phase, TiN, which extends from $TiN_{0.42}$ to $TiN_{1.00}$ (*28*). Comparison of the pyknometric density with that derived by X-ray methods leads to the conclusion that the cubic face-centered titanium lattice in $TiN_{0.42}$ is fully populated, but that the nitrogen lattice corresponding with this composition contains vacancies. For the stoichiometric composition both lattices have 4% of vacancies (*28*). In preparations with a nitrogen content up to $TiN_{1.16}$, the excess of nitrogen is readily lost by thermal dissociation and up to 20% of the titanium lattice sites are unoccupied (Section II,B,2) (*14*).

In addition to the above, an ϵ-phase exists, which has been little studied. The composition has been given as Ti_3N (*131*) or Ti_2N (*60*), and it is known to crystallize in an anti-rutile lattice (*60*), in which nitrogen is again surrounded by deformed octahedra of titanium atoms.

c. Vanadium. The solubility of nitrogen in cubic body-centered crystalline *vanadium* is very small at low temperatures. The γ-phase, VN, which again crystallizes in the NaCl lattice, has a narrower phase range than TiN (*15*, *32*, *33*, *53*). It also differs from TiN in having no appreciable concentration of lattice vacancies: pyknometric densities for the γ-phase agree very well with values deduced from X-ray measurements (*53*). The hexagonal intercalated phase is represented in this case by an intermediate β-phase, V_3N (*53*), whereas in the system titanium/nitrogen the same structure occurs as intercalated mixed crystals of α-Ti.

d. Chromium. The same intermediate phases occur in the system *chromium*/nitrogen. These are the cubic γ-phase, CrN, the stability range of which is unknown, and the hexagonal close-packed β-phase, Cr_2N (*11*, *34*, *135*). Cubic CrN is orthorhombically deformed below 0°C (*26*). This change is associated with the incidence of antiferromagnetism (cf. Section II,C,4,b). A hexagonal phase CrN has also been described, but cannot be considered as fully established (*137*).

e. Manganese. Phase studies in the system *manganese*/nitrogen (Fig. 5) are more extensive, although again not conclusive. The *tetragonal face-*

centered ϑ-phase, Mn_6N_5, is the richest in nitrogen. With increasing nitrogen content the ratio c/a approaches unity and extrapolation to MnN gives $c/a = 1$ (*107*). A cubic face-centered phase MnN has also been reported (*126*), although a lattice constant is given which it is impossible to reconcile with the extrapolation mentioned above.

As the nitrogen content is decreased, the η-phase, Mn_3N_2, appears. Its range of existence has been established, at least at low temperatures, and it is again *tetragonal face-centered.* Between it and the nitrogen-richer ϑ-phase there is a two-phase region in which the axial ratio c/a in the η-

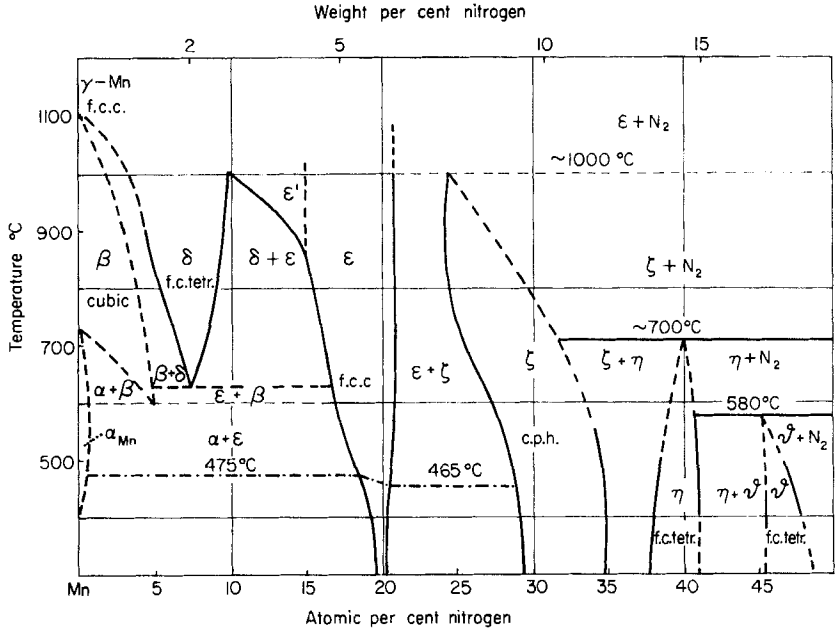

FIG. 5. The manganese/nitrogen system (*55, 87, 107*).

and the ϑ-phase alters with decreasing nitrogen content in the opposite sense (*49, 107*).

While the two tetragonal phases mentioned are structurally like the cubic MeN phases of Groups 3–6, it is found that, with lower nitrogen contents, a *hexagonal* ξ-phase with the composition Mn_2N occurs (*19, 49, 107*). The ranges of existence of the phases referred to above become narrower in all three cases as the temperature is increased.

An ϵ-phase follows which, at lower temperatures, has the composition Mn_4N and a small stability range (*49, 87*). Here a structure of the *perovskite* type (cf. Section A,II,1) occurs for the first time. At higher temperatures

the ϵ-phase region extends in the direction of lower nitrogen contents. An ϵ'-phase follows, which differs from the ferrimagnetic ϵ-phase in being paramagnetic (*87*). Extrapolation of the lattice constants of the ϵ- and ϵ'-phases gives the lattice constants of the cubic face-centered high-temperature γ-Mn phase (1095°–1134°C) (*87*). In the literature the Mn_4N phase is frequently described as having a smaller range and decomposing peritectically with rising temperature at 700°C (*55*). This would correspond with the behavior of Fe_4N, which will be discussed later, but the statement is very probably incorrect.

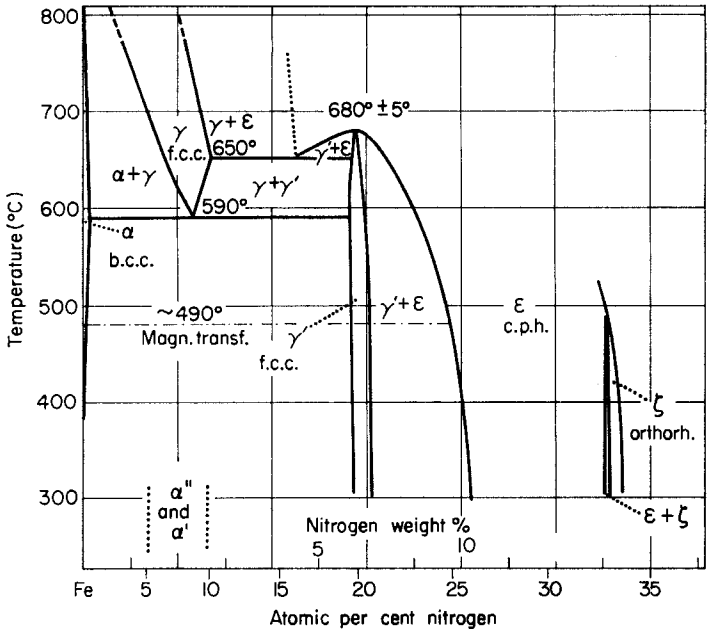

FIG. 6. The iron/nitrogen system (*55*, *70*).

With 4–10 atom% of N in a specimen that has been annealed at 1000° or 800° and very rapidly quenched, a *tetragonal face-centered* δ-phase is found (*49*, *87*). Its lattice constants would, with increasing nitrogen contents, approximate to those of the cubic ϵ-phase and, with decreasing nitrogen content—by extrapolation, to those of the tetragonal face-centered low temperature γ-Mn phase. There are thus close relationships between the γ-Mn high-temperature phase and the ϵ- and ϵ'-phases, and also between the γ-Mn low-temperature phase and the δ-phase.

There is also the possibility that a unique phase extends at high temperatures from high-temperature γ-Mn to Mn_4N; that is, γ-Mn is progres-

sively stabilized with increase in its nitrogen content, and exists as Mn_4N even down to room temperatures (*180*). On this basis Mn_4N is not an intermediate phase but a high-temperature γ-Mn mixed crystal. Occurrence of the δ-phase could then be attributed to incomplete stabilization at low nitrogen contents and to transition, notwithstanding very rapid quenching, to the tetragonal low-temperature γ-Mn phase.

f. Iron. The fact that the *iron*/nitrogen system is relatively well known is due particularly to the investigation of Lehrer (*106*), Eisenhut and Kaupp (*29*), and Jack (*67, 70, 71, 72*). For low concentrations of nonmetal there is an extensive analogy with the iron/carbon system.

Nitrogen has a low solubility in cubic body-centered α-iron. This reaches a maximum of 0.4 atom% N at 590°C. On the other hand, solubility in cubic face-centered γ-iron, which exists above 910°C, is high, and this phase is stabilized to lower temperatures by intercalation of nitrogen. The maximum nitrogen content is 10.3 atom% at 650°C and there is a eutectoid at 590°C, 8.75% N (*106*). Since the γ-phase corresponds with austenite in the Fe/C system it is called "*nitrogen austenite.*" With about 1 atom of nitrogen to 10 atoms of iron, about 10% of the octahedral holes of the cubic face-centered iron lattice are statistically occupied by nitrogen.

Further nitriding at higher temperatures, e.g., 700°C, leads at about 18 atom% N to the one-phase region of the ϵ-phase. This has a hexagonal close-packed arrangement of iron atoms with nitrogen distributed statistically in the octahedral holes. When a specimen of the hexagonal phase with 20 atom% N is cooled below 680°C a cubic γ'-phase Fe_4N results, while at somewhat lower nitrogen contents the ϵ-phase decomposes in a eutectoid reaction to the γ- and γ'-phases.

If nitrogen austenite (γ-phase) is cooled slowly it goes over eutectically to a mixture of the γ'-phase with α-iron. With quick cooling "*nitrogen martensite*" (α'-phase) is formed. In this, as in martensite, the iron atoms have a tetragonal body-centered arrangement. The nitrogen atoms are distributed statistically in the $\frac{1}{2}\frac{1}{2}0$ and $00\frac{1}{2}$ positions with a maximum of 9.4 N to 100 Fe (*70*).

When nitrogen martensite is annealed at somewhat over 200°C it is converted to $Fe_4N + \alpha$-Fe, just as martensite goes to $Fe_3C + \alpha$-Fe. When the annealing is done at a lower temperature (120°C), however, an intermediate α''-phase is formed which may be considered as an *ordered nitrogen martensite.* Its decomposition results only on prolonged annealing (*71*). The phase changes are represented in Fig. 7.

Figure 8 shows the structure corresponding to the ideal composition of ordered nitrogen martensite (α''-phase, $Fe_{16}N_2$). It is possible, however, for up to 50% of the nitrogen sites in the lattice to be unoccupied without change in the dimensions of the elementary cell. When iron atoms are

displaced in the direction of the *c*-axis, deformed octahedral holes (*71*) are formed from the holes of the original cubic body-centered or tetragonal body-centered elementary cell.

The structure of the α''-phase, $Fe_{16}N_2$, may also be derived from Fe_4N: each second Fe_4N-cell contains one nitrogen atom; tetragonal deformation of the elementary cell of Fe_4N is compensated by displacement of iron atoms in the direction of the *c*-axis, so that a true coordination number of 6 results (*71*).

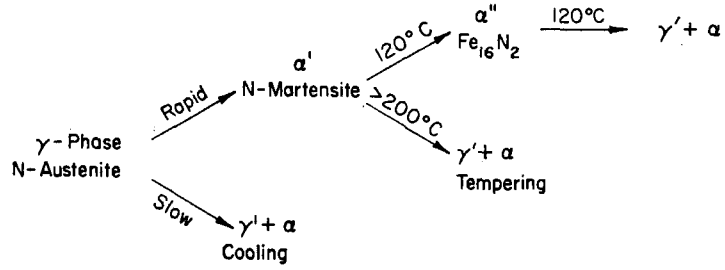

FIG. 7. Transitions of the γ-phase in the iron/nitrogen system at lower temperatures.

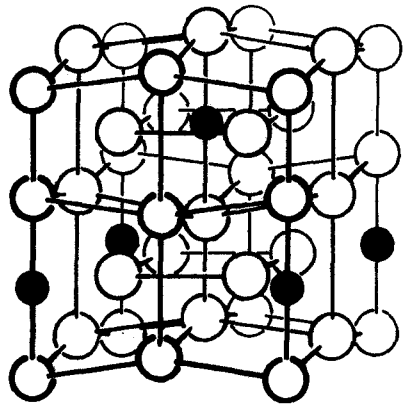

FIG. 8. Lattice of $Fe_{16}N_2$ (α''-phase of ordered nitrogen martensite): ○ Fe; • N.

The *hexagonal* ϵ-phase contains $Fe_2N_{0.66}$ in the unit cell when the composition is Fe_3N; this is valid for a statistical distribution of nitrogen atoms over the two available octahedral holes of the cell. In actual fact a superstructure (Fe_6N_2) of 3 times the volume with $a' = a\sqrt{3}$ is found. Figure 9(A) shows the positions of nitrogen atoms, according to Hendricks and Kosting (*57*), in the triple elementary cell with a lattice constant of $a\sqrt{3}$. Positions of the nitrogen atoms are shown. Iron atoms are shown only for the environment of one N atom with $z = 0$. They have $z = \frac{1}{4}$ or $z = -\frac{1}{4}$.

Nitrogen atoms are arranged so that neighboring octahedral holes are unoccupied in the direction of the *c*-axis and at right angles to it.

The hexagonal phase reaches almost the composition Fe_2N. In it there is the same superstructure cell; half of the octahedral holes corresponding to a composition that is somewhat poorer in nitrogen than Fe_6N_3 are occupied in such a way that there is a lattice vacancy above and below each nitrogen atom [cf. Fig. 9(B)]. In addition, there is one N atom in the "nitrogen layer" with $z = \frac{1}{2}$ and two in the other (with $z = 0$).

There is also an *orthorhombic* ξ-phase, Fe_2N, separated from this hexagonal phase by a very narrow two-phase region and with almost the

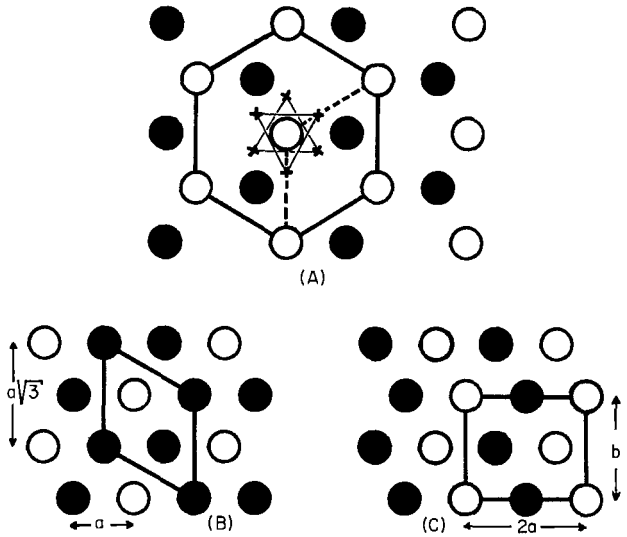

FIG. 9. Projections of the nitrogen sites on the x, y planes of iron nitride Fe_3N–Fe_2N. (A): ϵ-Fe_3N; (B) ϵ-Fe_2N; (C) ζ-Fe_2N; ○ N in $z = 0$; ● N in $z = \frac{1}{2}$; × Fe in $z = \pm\frac{1}{4}$.

same composition. The iron atoms in it have basically the same arrangement as in the hexagonal phase, but the orthohexagonal cell is somewhat deformed in the sense of becoming orthorhombic. Nitrogen atoms, however, are arranged differently. The two nitrogen layers referred to previously now each contain the same number of atoms. Figure 9(C) shows the structure of the orthorhombic elementary cell (Fe_8N_4). Neighboring octahedral holes are now filled by nitrogen in *one* direction, leading to an expansion in this direction compared with the original hexagonal form (*67*, *72*).

With intermediate nitrogen contents in the hexagonal phase, a superstructure with an even larger elementary cell makes its appearance as a result of ordered nitrogen layers. For the composition $Fe_{24}N_{10}$ the unit cell has $a'' = a \cdot 2\sqrt{3}$ for the same value of c.

g. Cobalt. In the system *cobalt*/nitrogen there is a similar situation: Co_3N is found as a hexagonal intercalated structure with a superstructure cell that has 3 times the volume (*25, 89*). With higher nitrogen contents this is succeeded by a broad two-phase region, followed by the stoichiometric phase Co_2N, having an orthorhombic deformed hexagonal close-packed arrangement like the ξ-phase of iron (*89*). Electron diffraction also reveals on cobalt surfaces a cubic phase, to which the composition Co_4N has been assigned, with a structure analogous to that of Fe_4N (*170*). A poorly crystallized CoN has also been described to which an NaCl structure (*154*) or, in more recent work, a zinc blende structure (*78*) has been attributed.

h. Nickel. In the system *nickel*/nitrogen there is a hexagonal Ni_3N phase of small breadth which, because of the ordered nitrogen layers, again requires a 3-fold increase in the unit cell size (*69, 90*). Electron diffraction has detected the Ni_4N phase (*169*), which is analogous to the case of cobalt. The nitride Ni_3N_2, formed by thermal decomposition of the amide, is amorphous (*173*).

i. Copper. It might be expected that this series would also include a corresponding nitride of *copper*. The compound Cu_3N has indeed been prepared, but has nothing in common with the nitrides of iron, cobalt, and nickel of the same composition. The compound shows no metallic conduction and crystallizes with the ReO_3 lattice. It must be considered as a compound of Cu(I) which is partly polar in character (*82*). It will not be further considered.

B. Preparative Methods

The most diverse methods are available for preparing metallic nitrides. This is due primarily to great differences in thermal stability and, associated with this, in enthalpies of formation. Thermal properties are described (Section II,C,1). It may be noted, however, that TiN, for example, has an enthalpy of formation of −79.7 kcal (*59*) and can be heated in nitrogen at 1 atm up to 2900°C. Both enthalpy of formation and thermal stability decrease with increase in the atomic number of the metal; Ni_3N has an enthalpy of formation of −0.2 kcal (*54*) and decomposes rapidly at 400°C. Indeed, this decomposition would occur at lower temperatures if it were not kinetically hindered.

In the following pages relevant preparative methods will be discussed with examples [cf. (*93*)], without, however, attempting a complete coverage of the literature.

1. Nitriding of Metals

This method is of the greatest importance today because metals of high purity are available.

(a) In nitriding with *nitrogen* it follows that only that phase will be obtained that is in equilibrium at the given temperature with the pressure of nitrogen used. The nitrides TiN (*1*, *28*), VN (*53*), and CrN (*11*) may be prepared with nitrogen at 1 atm. For complete nitriding it is necessary to employ temperatures between 1100° and 1600°C, depending on the fineness of division of the metal and the duration of the treatment. In the system manganese/nitrogen a nitrogen pressure of 1 atm at 750°C gives a product with about 22 atom% N (*153*) whereas, at 200 atm and 740°C, 32 atom% N is reached (*47*). In the case of elements of the eighth group, nitriding with nitrogen at pressures which can be attained without special facilities is no longer possible.

(b) A substantially higher degree of nitriding is attained by use of *streaming ammonia*. If ammonia at, say, 500°C is passed at a sufficiently high streaming rate over iron, it is found that the degree of dissociation in the gas phase is far short of the equilibrium value. Calculations from the equilibrium constant would indicate very high equilibrium pressures of nitrogen. In fact, the dissociation equilibrium in the gas phase is established slowly, whereas equilibrium between ammonia and metal, leading to the formation of nitride and hydrogen, is established rapidly. In this way it is possible from the metal and streaming ammonia to prepare nitrides of iron (*105*), cobalt (*89*), or nickel (*90*), all of which have a very low enthalpy of formation and also a very high equilibrium pressure of nitrogen at the temperature of their preparation.

A further preparative route is the use of a mixture of *ammonia* and *hydrogen*. With ammonia at 1 atm and for a given flow rate and temperature only a fixed nitrogen content can be attained. Variation in the volume ratio $NH_3:H_2$ in the gas taken enables lower nitrogen pressures to be set up, and this makes possible the preparation of less highly nitrided material. For example, a mixture of 98% NH_3 and 2% H_2, at 500°C and 1 atm, corresponds with a nitrogen pressure of about 8×10^9 atm, and a mixture of 70% NH_3 and 30% H_2 with a nitrogen pressure of about 1.2×10^6 atm (*36*). The formation of Fe_4N may be mentioned as an example. This requires an NH_3/H_2 mixture at 500°C with 20 vol% NH_3, corresponding with a dissociation pressure of about 5.2×10^3 atm N_2. This method of working has been important in establishing the Fe-N phase diagram (*105*, *132*).

2. Nitriding of Metallic Compounds

(a) The classical method for preparing metallic nitrides is the reaction of *metallic oxides*, e.g., TiO_2, with *nitrogen* in presence of *carbon*. This process was used in the fundamental researches of Friederich and Sittig (*40*), although it is applicable only to nitrides of high thermal stability and does not lead to pure products. With titanium, for example, reaction

above 1600°C with 1 atm N_2 leads to titanium carbide and, below this temperature, to titanium nitride. The ability of TiN to form mixed crystals with TiC and TiO also makes the thermodynamic treatment of the reaction very difficult (*117*). VN and CrN may also be made by this process, although contamination with carbide occurs even more readily.

(b) In many cases it has proved advantageous to nitride *amalgams, hydrides, oxides,* and *halides* with ammonia. The principle is well illustrated by the nitriding of manganese amalgam. As the temperature is increased the amalgam decomposes and the resulting very finely divided metal reacts with ammonia that is passing over it. This method may be operated at relatively low temperatures and yields products which are highly nitrided (*107*). Reaction with titanium hydride or vanadium hydride occurs similarly. They react with nitrogen or, better, with ammonia at 1000°C (*37*).

Ammonia has an additional role as a reducing agent in the conversion of oxides and halides. From NH_4VO_3 it is possible to make VN by reaction with ammonia at 900°–1000°C (*21*). Fe_3O_4 also reacts with ammonia at 430°C to form Fe_2N (*58*). Fluorides of cobalt and nickel, which have the advantage that they do not form ammines, are likewise reacted with ammonia (*89, 90*). Other halides may be transformed after intermediate formation of an ammine or following ammonolysis. Thus $TiCl_4$, for example, yields TiN of stoichiometric composition if the reaction temperature is increased to 1400°–1600°C (*14*). At lower temperatures material is produced with up to 20% of vacancies in the titanium sublattice, i.e., with an excess of nitrogen (*14*).

(c) Mention may also be made of experiments to prepare nitrides in the *plasma beam.* In a plasma burner fed with a mixture of 36 vol% N_2 and 64 vol% Ar, $TiCl_4$ is introduced with the nitrogen stream. Small crystallites of TiN separate in the cooled anode cavity. Since the elements are ionized in the beam the use of hydrogen may be dispensed with, although it is necessary in the growth process discussed below (*130, 165*).

3. Growth Processes

(a) The van Arkel process for the thermal decomposition of transition metal halides on a tungsten wire heated to a high temperature has also been used for making metallic nitrides. In preparing titanium nitride, $TiCl_4$ in an atmosphere of nitrogen and hydrogen is decomposed on a very thin tungsten wire heated electrically to 1000°–1400°C. Knowledge of the equilibrium underlying the reaction, which depends little on the temperature, allows the reaction temperature to be lowered still further. It is possible in this way to obtain 1–2-mm thick wires of TiN (*115, 117, 118, 171a*).

(b) Basically the same process is used to coat carrier materials such as steel or corundum with a thin surface layer of TiN (*24*). The temperature

may be lowered to about 1000°C and well adhering layers with thicknesses of 6μ, for example, may be obtained on sheet steel (*117*).

Using the same method, VN may be prepared from VCl_4, nitrogen, and hydrogen at 1400°–1600°C on tungsten wires (*115*), and VN layers may be put onto carriers at 1100°–1600°C (*24*).

4. Thermal Decomposition

(a) Thermal decomposition of metallic *nitrides* (also discussed in Section II,C,1) offers the possibility of preparing nitrides of lower nitrogen content by thermal decomposition of a highly nitrided product. Thus it is possible to submit Co_2N, which is the most highly nitrided compound, to careful degradation and so obtain Co_3N (*89*). Since, however, thermal decomposition is not generally done under equilibrium conditions, there is the danger of forming nonhomogeneous products.

(b) Nitrogen-rich nitrides may be prepared by thermal decomposition of *amides* obtained by precipitation from liquid ammonia. For example, CoN may be made from $Co(NH_2)_3$ (*154*) or Ni_3N_2 from $Ni(NH_2)_2$ (*173*). Equilibrium reactions are not involved and the products are not crystalline.

5. Reactions in the Solid State

(a) When stability relationships permit, preparations of medium nitrogen content may be obtained quite simply by heating the metal with a nitrogen-rich nitride. Reaction is favored by the use of fine grain sizes and pressing the mixed reactants. If sufficient attention is paid to homogenizing the material, this approach may be used in studying the systems titanium-, vanadium-, chromium-, and manganese-nitrogen.

(b) In this connection mention may be made of sintering and hot-pressing, a prerequisite of which is the production of material of small particle size by special processes. Temperatures of 1300°–1600°C and pressures of 70–150 kg/mm^2 are used. The process, which has long been of importance in laboratory and technical practice, is dealt with fully by Kieffer and Schwarzkopf (*94*). Contributions to the theory of sintering have also been made by Hüttig (*64*). The thermodynamics of the sintering process in the presence of carbon has been treated for TiN (*12*).

6. Melting

The preparation of nitrides in melts is not in general possible because the compounds either undergo thermal dissociation too readily or have very high melting points. The system titanium/nitrogen has been investigated with the aid of arc melting for products of low nitrogen content (*131*).

C. Properties

1. *Chemical and Thermal Properties*

Scandium nitride represents a bridge between polar calcium nitride and TiN, a typical transition metal nitride with metallic character. Saltlike nitrides are hydrolyzed by water with formation of ammonia, and this is true to a small extent of ScN. It is a strongly exothermic compound, although the only value for the enthalpy of formation, −67.5 kcal/mole (*125*), is an estimate based on interpolation. Collected values of enthalpies of formation and free enthalpies of formation are given in Table II. As for many transition metal nitrides, the melting point of ScN, 2627°C (*40*), is substantially higher than that of the metal (1400°C).

TABLE II
Thermodynamic Data

Phase	ΔH_{298} (kcal/1N)	ΔG_{298} (kcal/1N)	Reference	Additional readings
ScN	−67.5	—	(*152*)	—
TiN	−79.67	—	(*104*)	(*59, 63, 125*)
	—	−72.52	(*104*)	(*159*)
VN	−51.88	−45.7	(*112*)	—
γ-CrN	−29.01	—	(*104*)	(*124, 151*)
Cr_2N	−30.8	−24.2	(*111*)	—
ζ-$Mn_{2.5}N$	−24.1	—	(*110*)	(*160*)
ε-Mn_4N	−30.3	—	(*110*)	—
ζ-Fe_2N	−3.0	—	(*23*)	(*1, 70, 92, 120*)
γ′-Fe_4N	−4.5	—	(*23*)	(*22, 92*)
Ni_3N	−0.2	—	(*54*)	—
Cu_3N	+17.84	—	(*83*)	—

In *titanium nitride* the chemical properties of the transition metal nitrides as high melting cermets are well developed. Indeed, it has the greatest chemical and thermal resistance of any of the compounds in the series under consideration. In the cold it is attacked only by aqua regia but, on warming, slow attack occurs with acids or alkalies to yield ammonium salts or ammonia. TiN is resistant to chloride melts and metallic melts of iron, aluminum, or copper, but will not withstand oxide slags.

The scaling resistance in air is not very good. Systematic studies have shown that TiN in air undergoes a weight increase due to oxidation of 1 mg/cm² in 6 hours at 800°C. From kinetic studies it shows that two processes are operating at about the same rate: on scaling, rutile is being formed at the TiN/TiO_2 interface with an activation energy of 24.5 kcal/

mole, while oxygen and nitrogen diffuse through the rutile layer with an activation energy of 46.4 kcal/mole (*119*).

The enthalpy of formation of TiN determined by the Knudsen effusion method is $\Delta H_{298} = -79.7$ kcal/mole (*104*) and is the highest in the series of compounds under consideration. The same is true of the free enthalpy of formation ($\Delta G_{298} = -72.5$ kcal/mole) (*104*). In the effusion method, solid TiN vaporizes as titanium and nitrogen. With this method a nitrogen partial pressure of 32.2×10^{-6} atm is measured at 1968°C (*59*). Mass spectrographic studies also show that TiN is thermally dissociated at about 1800°C and does not evaporate as molecules (*2, 3*). The melting point, 2947°C (*1*), is particularly high. The sample must, of course, be melted in a nitrogen atmosphere as TiN dissociates in vacuum at high temperatures.

With increasing atomic number the chemical and thermal resistance of the nitrides decreases fairly steadily. *Vanadium nitride*, VN, is insoluble in nonoxidizing acids, but dissolves in either nitric or concentrated sulfuric acid. Part of the nitrogen appears as an ammonium salt and the remainder as elementary nitrogen. This behavior is also observed with the other nitrides. They are decomposed by strong alkalies with evolution of ammonia. V_3N is less resistant chemically than is VN (*53*). A value of 2050°C has been given for the melting point of VN, although it also undergoes decomposition (*40*). The enthalpy of formation of VN, determined by combustion calorimetry, is -51.88 kcal/mole (*112*), which is appreciably less than that of the preceding nitrides. The same is true of the free enthalpy of formation (-45.7 kcal/mole) (*112*).

The *chromium nitrides* CrN and Cr_2N dissolve in concentrated hydrochloric acid, part of the nitrogen being liberated as such. The enthalpies of formation of CrN and Cr_2N, determined by direct nitriding under pressure or by combustion calorimetry, are almost the same [CrN, -29.0 kcal/mole (*104*); Cr_2N, -30.8 kcal/mole (*111*)]. The free enthalpy of formation of Cr_2N is -24.2 kcal/mole (*111*). It is possible to prepare CrN with nitrogen at 1 atm, but melting points cannot be determined since CrN and Cr_2N decompose at about 1500°C without melting.

The *manganese nitrides* dissolve in dilute nonoxidizing acids with formation of ammonium salts and are also decomposed slowly by water. Enthalpies of formation are only a little lower than for the chromium compounds (ζ-$Mn_{2.5}N$, -24.1; ϵ-Mn_4N, -30.3 kcal/mole) (*110*). Equilibrium pressures are, however, substantially higher; the phase Mn_4N at 540°C has a nitrogen pressure of about 3 torr (*153*).

The *iron nitrides* are only slightly exothermic. Enthalpies of formation have been determined by solution calorimetry (ζ-Fe_2N, -3.0; γ'-Fe_4N, -4.5 kcal/mole) (*23*). The equilibrium between ammonia and iron leading to formation of the various iron nitrides and hydrogen has been studied

repeatedly (*31*, *132*). Equilibrium nitrogen pressures may be calculated from these experiments. It is found, for example, that Fe_4N at 525°C has a nitrogen fugacity of 5600 atm (*31*), a value which, compared with equilibrium pressure of Mn_4N already cited, illustrates the low stability of the iron nitrides. Nitrogen dissociation pressures have also been measured directly in high-pressure apparatus. The phases α-Fe and Fe_4N exist in equilibrium with one another at the following pressures: 300°C, 2100 atm; 400°C, 2300 atm; 500°C, 2700 atm. This is in approximate agreement with the results of phase analysis by the X-ray and magnetic methods and with the equilibrium measurements already referred to (*100*). At room temperature the iron nitrides are metastable; the rate of decomposition becomes measurable only at higher temperatures, which depend on particle size and nitrogen content.

A minimum in chemical and thermal stability is reached in the *nitrides of cobalt and nickel.* Ni_3N has an enthalpy of formation of -0.2 kcal/mole (*54*) and Cu_3N is actually endothermic with a value of 17.8 kcal/mole (*83*).

2. *Mechanical Properties*

The mechanical properties of nitrides are at least as important for their technical applications as chemical and thermal stability. It is not surprising therefore that this aspect of the subject has been studied intensively, particularly in the cases of TiN used as a metallic cermet and of the nitrides which are encountered in steel.

Scandium nitride, with a hardness of 7–8 on Moh's scale (*40*), is already decidedly hard. With *titanium nitride* a hardness almost equal to that of diamond is reached. The results of measurements are not, however, always concordant, and depend on the conditions of preparation and the purity of the specimens. With fused TiN, values of 9–10 (*37*) and 8–9 (*14*) have been recorded. Determinations of the microhardness of TiN layers evaporated onto steel gave Vickers hardness values of 1700–1900 kg/mm² (*117*). Titanium nitride is, however, extraordinarily brittle and as a result finds no uses as a cermet in its pure form. It may be sintered with a metal such as cobalt to give a satisfactory product or may be used as a surface coating. Compact TiN and evaporated layers of TiN on molded bodies may be polished with corundum powder (*117*).

Vanadium nitride, VN, is about as hard as TiN: values of 9–10 on Moh's scale have been found for specimens that have been melted (*7*, *40*). Comparative measurements of the microhardness on specimens subjected to varying degrees of nitriding and subsequently sintered have shown a relationship between the hardness and changes in bonding with progres-

sive nitriding ($VN_{0.338}$, 1900; $VN_{0.74}$, 1520; $CrN_{0.47}$, 1571; $CrN_{0.99}$ 1093 kg/mm^2) (*149*).

Reference may also be made to nitrided *chromium* surfaces, which are very hard and possess high thermal stability and corrosion resistance, as well as a high resistance to abrasion. They are characterized by microbrittleness, which hinders cold welding and seizing (*109*, *175*). These films find applications because of their corrosion resistance. Quite apart from nitride formation, incorporation of nitrogen in metallic chromium increases brittleness because of local distortions in the metal lattice. The cold brittleness boundary is also lowered as a result of local distortions in the chromium lattice (*96*, *174*). The influence of nitrogen is very much greater than that of oxygen (*172*).

The hardness of the *manganese nitrides* varies greatly. The ϵ-phase, Mn_4N, has a microhardness of 850–950 kg/mm^2 at room temperature (*6*). Above 700°C it becomes ductile and the ductility increases progressively as the nitrogen content of the ϵ-phase is decreased. The nitrogen-poor δ-phase obtained by quenching is also ductible, as is the low-temperature modification of γ-manganese itself (*87*, *180*). Manganese nitrides are also used as nitrogen-containing intermediate alloys in steel making.

There are no exact hardness measurements for the *iron nitrides* because sintered specimens cannot be prepared from them. Determinations of the microhardness of nitride deposits on iron gave the following values: nitrogen-containing α-Fe, 160; $\epsilon + \gamma$-phase, 280; nitrogen-martensite, 580; γ-phase 260 kg/mm^2 (*98*). A 0.5-mm thick nitride layer containing the α-, ϵ-, and γ-phases had a Vickers hardness of 927 kg/mm^2 (*138*).

These results show that the hardness of the iron nitrides is much below that of the nitrides so far discussed. In spite of this they are of considerable technical significance. This does not, however, depend directly on the properties of the iron nitrides. The hardness and other mechanical properties of nitrogen-containing iron obtained by surface nitriding are associated with iron lattice defects arising from nitride deposits; blocking of the glide planes results (*41*). Electron microscope studies also show that the hardness is due to deformation of the iron lattice resulting from nitride separation (*65*).

A further substantial increase in hardness is obtained by nitride formation in nitrided alloy steels. These contain particularly chromium, titanium, or vanadium, binary or ternary nitrides of which are produced in the process of surface nitriding. These phases, in conjunction with the effects associated with iron itself, produce the great hardness.

There is no information on the nitrides of *cobalt* and *nickel*, which cannot be obtained in the sintered form. It will be seen, however, that a

decrease in hardness is to be expected by analogy with the decrease in chemical and thermal stability in the nitrides from titanium to nickel.

3. Electrical and Optical Properties

All binary nitrides have a high *electrical conductivity*. This is often of the same order of magnitude as the conductivity of the pure metal and the temperature coefficient is always negative.

Scandium nitride, ScN, which may be considered as having a polar structure, has a small specific resistance (300×10^{-6} Ω cm). This value was obtained with a sintered specimen containing 4.5% Sc_2O_3 (*40*). TiN has the lowest specific resistance, with a value of 17.3×10^{-6} Ω cm, measured on rods of high purity made by the van Arkel growth process. The temperature coefficient of resistance is positive from 20° to 800°C (*117*). As the atomic number of the metal increases so does the specific resistance of the nitrides. For VN it is 200×10^{-6} (*40*), for $VN_{0.93}$ 85×10^{-6} (*149*), and for $VN_{0.338}$ 123×10^{-6} Ω cm (*149*). The specific resistances of $CrN_{0.926}$ (640×10^{-6}) and $CrN_{0.497}$ (79×10^{-6} Ω cm) differ sharply (*149*). Among the nitrides of the later elements in the series, only Ni_3N (2800×10^{-6} Ω cm) has been studied (*88*). Exact values cannot be obtained for nitrides of the eighth group as only powders are available for the measurements.

Cu_3N is a semiconductor; its electrical behavior shows that it does not belong to the transition metal nitrides (*88*). Measurements have also been made of the resistance of thin nitride films made by evaporation in the glow discharge in nitrogen, to which the formulas Fe_3N_2 and Ni_3N_2 have been assigned (*77*).

Superconductivity has been found in TiN below 4.2°K (*117*) or 5.6°K (*56*) and in VN below 8.2°K (*56*). The transition temperature in the case of TiN falls with increase in the oxygen content as a result of the incorporation of oxygen in the nitrogen sublattice. TiO itself is not a superconductor. A dependence on the oxygen content of the specimen is also observed in the case of VN if VN-VO mixed crystals are present (*56*). CrN does not show superconductivity down to 1.2°K (*56*).

The differential *thermoelectric coefficients* for the following nitrides have been measured: $TiN_{0.98}$ −10.8; $VN_{0.34}$ −5.3; $VN_{0.93}$ −4.6; $CrN_{0.50}$ −2.3; $CrN_{0.926}$ −92 μV/degree. All were examined in the sintered form (*149*).

Hall coefficients for the same five compounds were −0.67, −0.9, −0.45, −0.72, −264 cm^3/coul. (*149*). Trends in the values for the Hall coefficient, electrical conductivity, and thermoelectric coefficient of the nitrides have been correlated with the progressive filling of the 3*d* shell of the metal atom (*149*) (cf. Section II,D,2).

The *color* of nitrides varies greatly with the particle size. Powdered finely crystalline preparations are light brown (TiN), dark brown (VN), or

dark gray to black (nitrides from chromium to nickel). Well-crystallized specimens, made by the growth process (TiN, VN) or by sintering (TiN, VN, CrN), are golden yellow or bronze in color. They exhibit a metallic luster, which is enhanced by polishing. Recrystallized ScN, which is known only with a Sc_2O_3 content of 4.5%, is dark blue in color (*40*). Specimens of TiN containing oxide are likewise blue to blue-black (*40*). Materials prepared at relatively low temperatures from titanium tetrachloride and ammonia, which have a nitrogen content in excess of that corresponding to TiN and in which titanium is therefore present in part in an oxidation state of +4, are dark blue (*14*). In very thin transparent TiN films deposited on so-called "sapphire windows" consisting of ground Al_2O_3 plates, absorption has been measured in the range 200–1000 mμ. The absorption minimum is at 400 mμ. Contrary to what is observed visually, no difference is found between pure metallic TiN and semiconducting TiN containing oxygen (cf. Section III,A,3). The reflecting power in the infrared appears to be somewhat different for the two nitrides (*117*).

The *X-ray emission spectra* of some nitrides (TiN, VN, CrN, and Cr_2N) have been measured and compared with those of a large number of related compounds. The spectrum of TiN, for example, shows, in addition to the $K\beta_5$ line, a satellite at longer wavelengths which does not occur in the spectrum of titanium metal. The spectra of TiN, VN, CrN, and Cr_2N are explained by the splitting of the 3*d* level into t_{2g} and e_g levels by the crystal field in the octahedral environment (*123*).

The question of the charge on the nitrogen atom in intercalation compounds is difficult to answer. X-ray determination of the atomic scattering factor for nitrogen in Mn_4N shows that nitrogen is not an electron donor: results are consistent with N^0 or N^{1-}, but not with N^{3+}. The absence of low-angle reflections, from which the distinction between the different oxidation states is normally made, makes it impossible to differentiate between N^0 and N^{1-} (*103*). These results obtained by Kuriyama (*103*) do not agree with Elliott's determinations of the atomic scattering factor in Fe_4N (*30*), which show N^{3-} to be the probable species. They are, however, consistent with the general concept of a covalent metal-nitrogen bond (cf. Section II,D).

4. *Magnetic Properties*

In the transition metal nitrides one finds not only paramagnetism (e.g., in TiN) but also antiferromagnetism (CrN), ferromagnetism (Fe_4N, ϵ-Fe_2N), and ferrimagnetism (Mn_4N). Some of the compounds with the last three properties have been studied in very great detail as they are very important for theories of magnetism and the chemical bond (they are further discussed in Section II,D,2).

a. Paramagnetism. For nitrides of the type MeN, susceptibility values are known only in the case of TiN and CrN. Molecular susceptibilities, χ_{Mol} in cgs units, are

$$\begin{aligned} &\text{TiN (20°C)} \quad 89 \times 10^{-6} \ (97, 117) \\ &\text{CrN (24°C)} \quad 763 \times 10^{-6} \ (26) \end{aligned}$$

The paramagnetic susceptibility of TiN decreases somewhat with increasing temperature (*117*). CrN becomes antiferromagnetic below 0°C (cf. subsection *b*). Further susceptibility measurements on CrN and Cr_2N are difficult to correlate with those quoted (*122*).

The hexagonal ζ-phase in the system manganese/nitrogen (composition $MnN_{0.41}$) obeys the Curie-Weiss law of the form

$$\chi_{Mol} = \frac{0.0316}{T + 1070}$$

between $-180°$ and 530°C, leading to a value of χ_{Mol} for $MnN_{0.41}$ at 20° of 1405×10^{-6} (*179*). This gives a magnetic moment of 3.94 μ_B, which is only a little greater than that corresponding with the spin moment of three unpaired electrons. For preparations of the ζ-phase richer in nitrogen ($MnN_{0.48}$) and for the tetragonal η-phase ($MnN_{0.65}$), measured values are 949×10^{-6} and 784×10^{-6}, respectively (*18*).

The orthorhombic ζ-phase Fe_2N is also paramagnetic (*17*). The magnetic moment is 0.19 μ_B per Fe atom (*178*). The hexagonal ϵ-phase is normally ferromagnetic (cf. Section II,C,4,c), but nitrogen-rich specimens ($Fe_{2+x}N$, where $0 < x \leqslant 1$) have a low Curie point so that they are paramagnetic at room temperature (*17*).

A thermomagnetic study of the paramagnetic phase Ni_3N has yielded information on its decomposition temperature. It has also been found that nickel formed in the decomposition has a Curie point that is lowered by about 18° because of intercalated nitrogen (*9*).

b. Antiferromagnetism. The only antiferromagnetic nitride identified so far is CrN below 273°K, which has been fully studied. Following the increase of susceptibility with decreasing temperature, there is a sharp drop in susceptibility at the Néel point of about 273°K. The structure of antiferromagnetic CrN is derived from that of the paramagnetic high-temperature modification (NaCl type) by orthorhombic deformation of the original cubic elementary cell. The orthorhombic *a*- and *b*-axes result from the face diagonals of the rock salt lattice, while the orthorhombic *c*-axis corresponds with the cubic axis. Figure 10 shows the structure. Only the Cr positions are shown, with $z = 0$ as points and $z = \frac{1}{2}$ as circles. The crystallographic orthorhombic elementary cell is shown by dotted lines, and the relationship to the original cubic elementary cell is also

indicated. One of the diagonals of the cubic face (a_{rh}) is shortened by about 1% and the other ($2b_{rh}$) is lengthened by the same amount. Alternating two (h00) planes are moved somewhat nearer together, as indicated by brackets in the diagram.

Neutron diffraction photographs at 77°K show a magnetic superstructure with 4 times the volume of the crystallographic cell; the *a*- and *b*-axes have to be doubled. Figure 10 also indicates the arrangement of spins. All spins lie parallel to the rhombic *b*-axis. In CrN we have one of the two possible "antiferromagnetic structures of the fourth order" (*26*). The spin moments of the atoms of *one* rhombic (h00) plane are all parallel. The

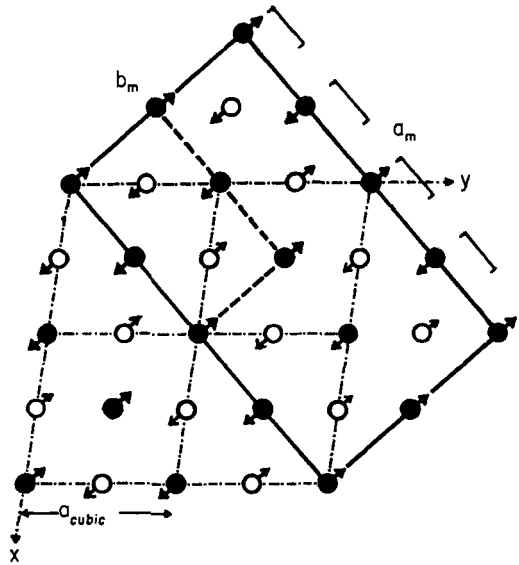

FIG. 10. Projection of chromium sites of antiferromagnetic CrN on the *x*, *y* planes: ○ Cr in z = ½; ● Cr in z = 0.

resulting moments of these planes are, as one progresses in the [100] direction, arranged in the sequence $++--++--$. The interaction of the planes is thus alternately ferromagnetic and antiferromagnetic in type.

c. Ferromagnetism. Binary ferromagnetic transition metal nitrides are so far known only in the system iron/nitrogen. Ternary ferromagnetic nitrides may also be derived from them (cf. Section III,A,1).

Hexagonal ε-iron nitride at low temperatures is ferromagnetic over the whole phase range, but at room temperature only specimens with a low nitrogen content exhibit this property. The Curie point rises from −200°C for $Fe_{2.05}N$ to +270°C for $Fe_{2.8}N$ (*106*). The magnetic moment per iron

atom, obtained from saturation measurements, rises in the same sense. Following the paramagnetic rhombic ζ-Fe_2N phase, the moment at first rises sharply, then more slowly, until in the region from $Fe_{2.1}N$ to $Fe_{2.5}N$ the rise is linear from 1.1 μ_B to 1.9 μ_B. It remains constant from $Fe_{2.5}N$ to Fe_3N (*178*). Since the nitrogen content is related to the lattice dimensions, both the Curie point and the magnetic moment may also be represented as a function of the lattice dimensions (*17*).

The magnetic structure of a specimen of the ϵ-phase with the composition $Fe_3N_{1.17}$ ($Fe_{24}N_{9.36}$) has been studied in detail by Robbins and White (*139*). The hexagonal unit cell determined by X-rays contains in the ideal case 24 Fe atoms and 10 N atoms (cf. Section II,A,2,f). Since the distribution of N atoms in the octahedral holes has no bearing on the magnetic structure, the description of the arrangement of spin vectors for the metal atoms requires only a unit cell containing two Fe atoms. The following expressions describe the relationships between the axes of the two unit cells: $2a_{magn}\sqrt{3} = a_{cryst}$; $c_{magn} = c_{cryst}$. From neutron diffraction observations, the spin moments of the Fe atoms all have the same orientation and are parallel to the *c*-axis: this means that the compound is ferromagnetic. Neutron diffraction gives a moment of 1.5 μ_B per iron atom and extrapolation of the magnetization curve to 0°K gives 1.33 μ_B (*139*). This low value has been taken as proof that nitrogen is acting as an electron donor. The same conclusion is reached from structural data, for, taking the radius of the iron atom as 1.26 Å, that of nitrogen is found to be 0.66 Å. This is considerably smaller than the radius of $N^{\pm 0}$, which the authors take as 0.77 Å (*139*).

The *cubic γ'-phase*, Fe_4N, has also been fully studied. The Curie point for the stoichiometric composition Fe_4N is at 488°C (*46*). Between $Fe_4N_{0.97}$ and $Fe_4N_{1.04}$, which is the region of the γ'-phase, the Curie point varies from 481° to 508°C (*17*). Fe_4N has a magnetic moment of 8.86 μ_B per unit formula at 0°K (*46*). The mean value per atom of Fe agrees with that for α-Fe (2.22 μ_B) (*161*). On the basis of saturation measurements, Wiener and Berger have given an interpretation of the magnetic structure of Fe_4N which is also supported by measurements on the ternary compounds Fe_3NiN and Fe_3PtN (cf. Section III,A,1) (*176*). Frazer (*39*) has verified the structure proposed by neutron diffraction: iron atoms in the corners of the cube (cf. Fig. 11) have spin moments that are parallel to one another; the moment per Fe_c is 3 μ_B. A second magnetic sublattice is formed by the three face-centered iron atoms; the moment per Fe_f is 2 μ_B. The interaction between these two sublattices is also ferromagnetic. This model has also been verified by NMR studies with $_{57}Fe_4N$ (*4*). The relationship of the magnetic moments could also be established by interpreting the Mössbauer effect for Fe_4N (*158*).

d. Ferrimagnetism. The Curie point for the stoichiometric composition Mn_4N is at 483°C, and over the range $Mn_4N_{1.04}$ to $Mn_4N_{0.77}$ varies from 473° to 513°C (*86*). Measurements of saturation magnetization with Mn_4N gave a magnetic moment of 1.14 μ_B per unit formula at 0°K, corresponding to a mean moment of 0.3 μ_B per Mn atom (*47*, *86*). Guillaud and Wyart recognized that the low moment of manganese was due to a partial paral-

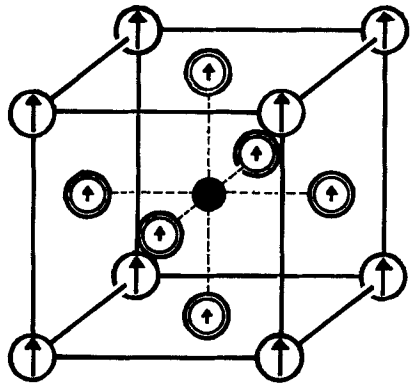

FIG. 11. Magnetic structure of Fe_4N: ○ Fe_c; ◎ Fe_f; • N.

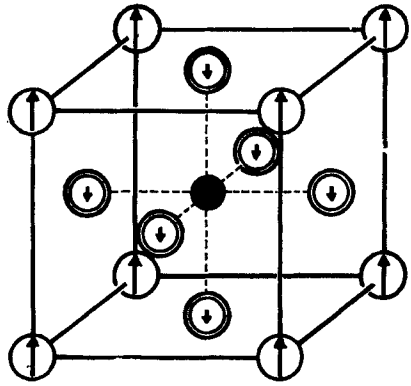

FIG. 12. Magnetic structure of Mn_4N: ○ Mn_c; ◎ Mn_f; • N.

lel—or antiparallel—arrangement of the spin moments, that is, to an uncompensated antiferromagnetism (*47*), which Néel (*121*) has termed ferrimagnetism. More certain indications of the magnitude and direction of the moments at the Mn positions were obtained in studies with polarized neutrons at 77°K (*167*, *168*). Manganese atoms at the corners (Mn_c) and those at the centers of faces (Mn_f) both form a magnetic sublattice (cf. Fig. 12). Within the sublattice there is a ferromagnetic coupling of the

spin moments, and the moments between the two sublattices are coupled antiferromagnetically. For Mn_c and Mn_f the moments are $+3.84\ \mu_B$ and $-0.90\ \mu_B$, respectively. The residual moment of $+1.14\ \mu_B$ per Mn_4N gives rise to ferrimagnetism (cf. Section II,D,2).

D. Bonding in Transmission Metal Nitrides

There is as yet no complete theory of bonding in transition metal nitrides. Concepts developed up to the present are based essentially on intercalation compounds of the types MeN, with the NaCl structure, and Me_4N, with the perovskite structure. Two approaches are apparent, one based mainly on the theory of the covalent bond and the other on the band theory of bonding in metals. The latter has been extended by inclusion of elements of the covalent bond model.

1. Covalent Model

Pauling (*133*, *134*) explains bonding in the above two groups of nitrides in terms of his theory of the metallic bond, which he considers to be closely related to the covalent bond. Each atom of a metal forms covalent bonds with the neighboring atoms. Since the number of these is greater than the number of electron pairs available for covalent bonds, resonance occurs between the possible canonical forms. The electrical conductivity of metallic substances is based on this resonance.

Pauling's system of metallic valency and metallic single-bond radii R(1), together with the bond number n (the quotient of the number of electron pairs available for bonds and the number of possible canonical forms), makes it possible by using the relationship

$$R(1) - R(n) = 0.300 \log n$$

either to calculate the *lattice dimensions* R(n) from tabulated single-bond radii, assuming reasonable bond numbers, or, using X-ray determinations of the lattice dimensions, to calculate and interpret the bond order.

Applying these concepts to nitrides, it is assumed that nitrogen has the $2s$ orbital and three $2p$ orbitals available for bonding. Bonding in the NMe_6 octahedra is brought about by the five valency electrons of nitrogen and 6/2 electrons of the neighboring metal. This gives a bond order $n = 4/6$, i.e., four bonds distribute themselves by resonance over six canonical forms. As an example, in vanadium nitride each vanadium atom has, after forming bonds to nitrogen, two further electrons that are available for the vanadium-vanadium bond. The bond order in the cubic face-centered vanadium sublattice is accordingly $n = 2/12$, when electrons of the neighboring atoms are taken into account.

Calculation of interatomic distances by the use of Pauling's single-bond radius of 0.70 Å for the nitrogen and the bond order referred to above leads, in the case of vanadium nitride, to good agreement with the values found by X-ray analysis. This method of calculation fails, however, when applied to ScN, TiN, and γ-CrN. Systematic deviations occur, depending on the atomic number of the metal. Thus in ScN and TiN the calculated Me-Me distances are too large and in CrN they are too small. Calculation of the bond order from distances based on X-ray analysis likewise yields results which are only qualitatively useful. In the case of Me_4N results are equally inexact. In spite of these large deviations, later authors have continued to use the basic concept of resonance in the covalent bond between nitrogen and the transition metal and of the multiple canonical forms in resonance for the covalent bonds between metal atoms.

Rundle's model (*142*) is a development of that proposed by Pauling. He limited his treatment to intercalation compounds of the type MeN and MeC with a rock salt structure formed by transition metals of Groups 3–5. However, he introduced additional postulates about the hybridization on both the nonmetal and the metal. It was concluded, on the basis of the increased Me—Me distance in the cermets compared with that in the pure metals, that electrons were withdrawn from the Me—Me bonds and used in Me—N bonds. High melting points were explained by Rundle in terms of strong Me—N bonds, and both hardness and brittleness were associated with the presence of directed covalent bonds.

The preferential occurrence of the NaCl structure with its octahedral coordination is due to use of the three nitrogen p orbitals which are at right angles to one another. The two electrons in the nitrogen s orbitals do not in most cases participate in bonding, so that six *half-bonds* are formed from the metal to nitrogen and the bond order $n = \frac{1}{2}$. The metal atom has hybridized d^2sp^3 orbitals available for bonding to nitrogen. If the nonmetal is less strongly electronegative with respect to the metal, sp hybridization occurs on the nonmetal so that two two-electron bonds and four half-bonds can be formed by using both the remaining $2p$ orbitals. The bond order n is then equal to $\frac{2}{3}$. Whether $n = \frac{1}{2}$ or $\frac{2}{3}$ can be estimated from the Me—N distances. For $n = \frac{1}{2}$ the Pauling single-bond radii will be exceeded by $\sim$0.18 Å and for $n = \frac{2}{3}$ by $\sim$0.10 Å. This distinction is, however, somewhat too rigid. Electrical conductivity is attributed to bond resonance as in the Pauling model.

Hume-Rothery (*61*), in contrast to Rundle, considers the arrangement of metal atoms as the factor determining the occurrence of an NaCl structure for nitrides of the type MeN. Nitrogen enters preferentially the octahedral holes in the cubic close-packed metal atom lattice, but not those in the hexagonal close-packed lattice. According to Hume-Rothery, the

environment of the metal atom is a determinative factor as well as the electron-deficient bonds based on the three $2p$ orbitals of nitrogen. In the NaCl type, d^2sp^3 hybridization allows octahedral coordination of nitrogen around the metal atom, whereas in the hexagonal close-packed metal lattice the metal atoms would be surrounded by nitrogen atoms in a trigonal prismatic arrangement. This arrangement is not observed for the nitrides in Groups 3–5.

The drop in melting point in going from TiN to VN is believed to be due to weakening of the bonding with increase in the electron concentration, as was also suggested by Rundle.

Samsonov has made a detailed study of the effect of electron concentration on bonding in cermets (*145*, *146*). He considers the nitrides as intercalation compounds with metallic character, in which isolated atoms of nonmetal are intercalated in the metal lattice. For one and the same nonmetal, bonding is then determined by the extent to which the incompletely filled d shell of the transition metal atom is occupied and by its position in the Periodic Table. The possibility of electron transfer from the nonmetal to the vacant orbitals of the metal atom is then expressed in terms of the "acceptor ability," $1/N_d n_d$, where N_d is the principal quantum number of the partly filled d shell, and n_d the number of electrons in this shell. It will be seen that the acceptor ability decreases with increasing atomic number. Various properties of the material vary systematically with the magnitude of this quantity. For example, with decreasing acceptor ability, for a certain number of intercalation compounds of Groups 4–6 there is a decrease in electrical conductivity (*148*), heat of formation, lattice energy (*123*), and hardness (*123*).

The treatments of Pauling, Rundle, and Hume-Rothery involve only σ-bonds between the metal and nitrogen in which the two e_g orbitals of the metal participate. Krebs (*99*) has suggested a resonance system of π-bonds between the three p orbitals of nitrogen and the t_{2g} orbitals of the metal, and this also should provide an explanation of the occurrence of the NaCl structure and of electrical conductivity.

A more precise application of the concept of the covalent bond to intercalation compounds of the type MeN and MeC is due to Bilz (*10*), who treated isolated XMe_6 coordination polyhedra within the lattice as "XMe_6 molecules" and provided a molecular orbital scheme of their bonding. Only σ-bonds were discussed. In each Me only that of the six d^2sp^3 hybrid orbitals is considered which is oriented toward the central nonmetal atom and is almost completely localized in this direction. Molecular orbitals involving the s orbital of the nonmetal and the corresponding metal orbitals gave little localized $\frac{1}{6}$-bonds, whereas molecular orbitals from p orbitals of

the nonmetal and the corresponding metal orbitals are localized half-bonds. This provided a more precise picture of Rundle's $\frac{2}{3}$-bonds.

Metal-metal bonds were not taken into account in the molecular model. Bilz therefore tried to broaden the concept of the pure molecular model by introducing the separate "XMe_6 molecules" into the lattice so that the orbitals overlapped. In the authors' view, the covalent model expanded in this way by introducing elements of the band model is still unsatisfactory.

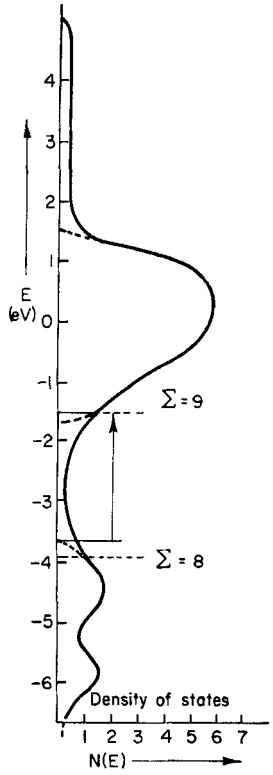

FIG. 13. Band scheme of TiN and TiC (*10*).

2. Band Model

Bilz (*10*) appended to his discussion of the covalent model a calculation of the electronic states for cermets MeX, based on the band theory of metals. The calculation was made for the [100], [111], and [110] directions in the K-space. From this the pattern of density of states was derived (cf. Fig. 13).

The low-lying p-band with strongly oriented *eigen* functions below the Fermi limit for Σ(valency electrons) = 8 (TiC or ScN) corresponds with the valency bond in the covalent model. The metallic bond corresponds to the very broad s-band with a low density of states which overlaps both the narrow p-bands, with a higher density of states, and the d-band, the functions of which are less dependent on direction. It is therefore to be expected that the metallic character will increase with increased electron occupation of the d-band in the series ScN, TiN, VN. This is supported by Kume and Yamagishi's nuclear magnetic resonance measurements on ScN and VN (*102*), which reveal more metallic character for VN and show ScN to resemble a half-metal. Presumably this may be correlated with the more polar character of ScN. The increase in metallic character required by Bilz's treatment is not, however, shown in the trend of electrical conductivities.

Between the p- and d-bands there is a marked minimum in the density of states at the Fermi boundary of Σ(valency electrons) $\simeq 8.5$. According to Bilz, this minimum is essential for comparing the band model with the observed properties of the materials: directed bonding of the p-band determines hardness and band overlapping the electrical conductivity. The latter becomes higher the higher the Fermi boundary lies. It is possible in this way to explain why the specific conductivity of TiN is greater than that of TiC. In the system TiC/TiN a minimum in conductivity in passing through the Fermi boundary would be expected as a result of a minimum density of states at about the composition $TiC_{0.5}N_{0.5}$. Experimentally, a conductivity minimum is found for the composition $TiC_{0.25}N_{0.75}$ (*108*). On the same basis a mixed phase $TiC_{0.5}N_{0.5}$ should show a melting point maximum with respect to its components TiN and TiC (*1*).

Incomplete occupation of the lattice of a cermet, which is often observed, especially among nitrides, is explicable in terms of a tendency to lower the Fermi boundary as far as possible below Σ(valency electrons) = 8.5. This allows extensive occupation of only the p-states. The light absorption of TiN and the color change of TiN/TiC mixed crystals with increase in the TiC content have also been correlated with the special Fermi boundary of Σ(valency electrons) = 8.5 (*10*).*

In describing bonding in nitrides with the rock salt or perovskite structure, Goodenough (*44*) starts from the metallic bond in transition metals. According to Mott (*116*), the distribution of electrons between the localized and the more delocalized bonding states is determined by a critical distance R_c: when the distance of the transition metal atoms in the lattice exceeds this value, the electrons are localized. When R_c is not exceeded "collective" electrons are present. Goodenough (*43*) gives a value of $R_c \lesssim 2.9 \pm 0.1$ Å. In the face-centered cubic metals Ni and Co, for example, the distance to

* New discussion of band structure of TiC, TiN, and TiO (*34a*).

the twelve nearest neighbors, $R_{nn} \sim 2.5$ Å, which is $< R_c$. That to the six next-nearest neighbors $R_{nnn} \sim 3.5$ Å, i.e., $> R_c$. Bonding to the next-nearest neighbors occurs through e_g orbitals (d_{x2-y2}, d_{z2}), i.e., through extensively localized electrons which are in directed bonds involving narrow bands with a high density of states. Bonding to nearest neighbors is through t_{2g} orbitals (d_{xy}, d_{xz}, d_{yz}), which give a broad t_{2g}-band. There is also a very broad band with a low density of states which is formed by s and p orbitals. It is in these two bands that the collective electrons are found. A band scheme has been proposed for the cubic face-centered metals, Mn, Fe, Co, and Ni (*43*).

Nitrides with a *rock salt* structure were described by Goodenough as "ionic compounds with metallic conductivity" and in particular related to the oxides (*44*). In these compounds the band is partly ionic in character, because of the electronegativity difference between metal and nitrogen, and also partly covalent. Electrical conductivity is associated with partial filling of the t_{2g}-bands by collective electrons and is limited to compounds in which the metal-metal distances are less than R_c (as is the case for nitrides).

Nitrides crystallizing in the sodium chloride lattice are then formed only if three or less d electrons are available in the formally trivalent cation, so that the e_g orbitals are empty and the t_{2g} orbitals are either half or less than half filled. With large differences in electronegativity there is a large forbidden zone and the bonding electrons belong largely to the nitrogen sublattice; the bonding s and p-e_g electrons are predominantly on the nitrogen (ScN). With decreasing electronegativity difference the bonding electrons take on a stronger e_g character. The increasing covalent character of the bond may lead to cation-anion-cation exchange interaction (e.g., CrN).

Special bonding relationships intermediate between the two extremes described above exist in *γ-chromium nitride*, CrN. This modification, which crystallizes in the NaCl lattice and is stable at room temperature, has a magnetic moment corresponding essentially with the spin-only value for the Cr^{3+} ion. The covalent part in the bonding is not localized. Below 0°C CrN is antiferromagnetic with the magnetic structure given (Section II,C,4,b) (cf. Fig. 10). Transition from cubic to orthorhombic symmetry is associated with localization of the covalent bond. Cations in the (h00) planes (orthorhombic indication) have spin moments that are parallel to one another. In the [100] direction the spin arrangement for the (h00) planes alternates (cf. Fig. 10).

The covalent part of the Cr—N bond is now localized in the direction of the z-axis. Formation of a Cr—Cr bonding band occurs through d_{xz} and d_{yz} orbitals, which are inclined at 45° to the c-axis and are directed toward the neighboring Cr atoms (x and y being the axes of the original cubic lat-

tice). The magnetic arrangement is as follows: cation-anion-cation interactions along the z-axis are ferromagnetic, but are antiferromagnetic within a (00l) plane. Cation-cation interaction between cations that are close together and bonded by d_{yz} and d_{zz} orbitals is antiferromagnetic, while for those which are more separated it is ferromagnetic. The d_{xy} orbital is not involved in bonding (*42*).

Nitrides of the *perovskite* type Me_4N are classified by Goodenough as interstitial alloys (*44*). The Me—N bond in these substances is predominantly covalent in character, i.e., nitrogen is probably present in the lattice as a neutral atom. The concept of a covalent metal-nitrogen bond accords with Kuriyama's determination of the atomic scattering factor of nitrogen in Mn_4N (*103*) (cf. Section II,C,3), which shows nitrogen to be present as either N^0 or N^{1-}. Nitrogen has the $2s$ orbital and three $2p$ orbitals available for bonding, as in nitrides of the type MeN, and the metal has the e_g and t_{2g} orbitals. Me_c—Me_f, the distance between metal atom nearest neighbors (M_c is the metal atom at the corner of the cube and M_f that in the center of a face), is far below the critical distance. These bands therefore involve a broad t_{2g}-band containing collective electrons. As a result, good electrical conductivity is observed. In considering bonding to the next-nearest neighbor metal atoms two cases arise: bonding of the type Me_c—Me_c occurs through localized electrons in the e_g-band, and that of the type Me_f—N—Me_f, involving metal atoms in the centers of cubic faces, occurs via nitrogen atoms.

In the bonding Fe_f—N band of ferromagnetic *γ'-iron nitride*, Fe_4N (cf. Section II,C,4,c and Fig. 11) there are spin-paired states involving a p electron of nitrogen, so that only one e_g electron per Fe_f can contribute to the atomic moment. A further contribution comes from an unpaired t_{2g} electron, so that Fe_f has a moment of 2 μ_B; 0.95 electron is given up to the 4s-band. Fe_f—N—Fe_f interactions are all ferromagnetic and, in this way, a magnetic Fe_f sublattice comes into being. A second sublattice involving Fe_c also has spins which are parallel. The atomic moment of Fe_c is 3 μ_B, i.e., 1 μ_B more than that of Fe_f, because the absence of spin pairing with a p electron of nitrogen produces an increase in moment. Interactions between the two sublattices Fe_f and Fe_c are also ferromagnetic in character. The ferromagnetic interaction of the two sublattices is explained by Goodenough's rule (*43*, *44*). This states that ferromagnetic coupling between the sublattices of a cubic face-centered arrangement of metal atoms will occur if n, the number of t_{2g} electrons, is greater than 5 but equal to or less than 6. This is true here as the 4s-band of iron has 0.95 electron per iron atom and there are two electrons in the e_g-band.

Following the neutron diffraction study of *ε-manganese nitride*, Mn_4N, by Takei *et al.* (cf. Section II,C,4,a) (*167*, *168*), Mekata (*114*) has given a

qualitative band scheme for this substance. It is a modification of Goodenough's scheme for cubic face-centered manganese, but differs in the energetic arrangement of the e_g- and t_{2g}-bands relative to one another.

This scheme, shown in Fig. 14, relates to manganese (Mn_c) at the corner of the unit cell (Fig. 14a) and at the center of faces (Mn_f) (Fig. 14b) Mn_c forms one of the magnetic sublattices and the three Mn_f atoms the other. Spin moments of the two sublattices are antiparallel to one another. This is in agreement with Goodenough's rule, according to which antiferromagnetic coupling of the sublattices occurs if the number, n, of t_{2g} electrons is greater than 3 but not more than 5 (*44*). The diagram takes

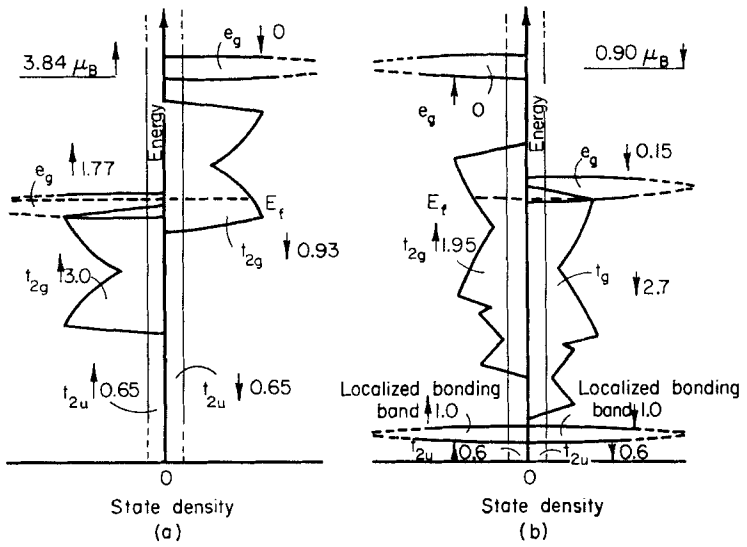

FIG. 14. The schematic state density curves of the energy bands in Mn_4N: (a) corner site Mn, and (b) face-centered Mn (*114*).

into account experimentally determined values of 3.84 μ_B for Mn_c and 0.90 μ_B for Mn_f.

The degree of occupation of the sub-bands is usually different for the two directions of spin (drawn in each figure to left and right) since these are displaced energetically relative to one another. Intraatomic exchange increases with localization of the electrons. Consequently the displacement is greater for the e_g sub-band than for the t_{2g} sub-band.

The scheme shows that from Mn_c there is a broad t_{2g}-band with a low density of states to the next manganese neighbor (Mn_f), this band being occupied by "collective electrons." The number of electrons in the t_{2g}-band is shown in the figure, account being taken of the spin orientation. A narrow

e_g-band with a high density of states is also present. This is directed toward the next-nearest neighbor manganese, i.e., from Mn_c to Mn_c. A very broad t_{2u}-band, made up from 4*s* and 4*p* orbitals and occupied by electrons with oppositely directed spins, overlaps the other bands. The density of states in this band is very small and it is shown on a much larger scale.

The band scheme for Mn_f is shown on the right. The low-lying narrow e_g-band with a high density of states brings about bonding between Mn_f and nitrogen. One of the two electrons is supplied by nitrogen. There are three electron pairs available per nitrogen atom and these have to participate in six bands. They correspond with the half-bonds postulated by Rundle (*142*) (cf. Section II,D,1). The t_{2g}-band is broader than for Mn_c because the site symmetry of Mn_f is tetragonal with each Mn_f enclosed by two N atoms. Mn_c and Mn_f are also not equivalent, so that the crystal field acting on Mn_f has tetragonal symmetry. The t_{2g}-band again serves to bond the manganese atom to the nearest neighbor at the corner of the cube, i.e., Mn_f to Mn_c.

III. Ternary Compounds

The binary compounds that have been discussed are all members of a single group. More recently many investigations have been made in which the influence of a third element, either metallic or nonmetallic, in combination with binary nitrides has been examined. Ternary compounds are obtained which belong to very different classes of substance.

If a transition metal is partly exchanged for a neighboring transition metal, the properties of the ternary compound differ little from those of the binary nitride. Introduction of one of the b-group metals has a significantly greater effect.

Partial substitution of nitrogen by carbon or oxygen may change the properties of the starting material to a greater extent than substitution of the metal by a neighboring transition metal. This is related to the strong influence of the nonmetal on the nature of the bonding in the interstitial alloy.

Quite different products, which are polar in character, are formed if the third component is a very base metal or a strongly electronegative nonmetal. The classification adopted in the following pages is based on these general considerations.

A. Ternary Metallic Phases

1. Double Nitrides

a. Mixed Crystals of the NaCl Type. The close relationship between binary nitrides that crystallize in the sodium chloride lattice leads to the

expectation that a range of mixed crystals will be formed. They may in fact be prepared from mixtures of the nitrides by hot-pressing in a nitrogen atmosphere at 2000°–2400°C (*27*, *128*). Alternatively, alloys may be nitrided with ammonia at 650°–950°C (*157*). In binary combinations of TiN, VN, ZrN, and NbN complete miscibility is always observed, except in the system VN/ZrN where the lattice constants of the binary components differ markedly. Lattice constants in the mixed crystal ranges show only a small positive deviation from Vegard's rule. TaN, which is irregular in that it crystallizes in the hexagonal system, does not display unlimited solubility in the above nitrides. Metals of the first transition series may be replaced by tantalum only up to the limits $Ti_{0.9}Ta_{0.1}N$, $V_{0.75}Ta_{0.25}N$, and $Cr_{0.75}Ta_{0.25}N$ (*157*).

Study of these mixed crystals shows that their properties are by no means always additive. In the comparable system TiC/VC a study of the Hall effect has revealed that the density of charge carriers does not increase linearly with the vanadium content, but passes through a well-defined maximum. The number of conduction electrons increases from about 0.2 for TiC, through a maximum of about 1.8 to 1.2 for VC. This observation may be explained in terms of a disturbance of the lattice periodicity of the titanium-vanadium alloys. The strict band model is no longer adequate to explain the effect. There is no such disturbance of lattice periodicity when carbon is replaced by nitrogen (cf. Section III,A,2) in the system TiC/TiN, in which the number of conduction electrons increases only a little from TiC to $TiC_{0.5}N_{0.5}$ and then rises more rapidly and linearly with the nitrogen content (*66*).

b. Hexagonal Phases. The metals Mn, Fe, Co, and Ni are able to replace tantalum partially in the hexagonal lattice of ϵ-tantalum nitride, TaN. The compounds Ta_3MnN_4, $\sim Ta_2FeN_{2.5}$, $\sim Ta_2CoN_{2.5}$, $\sim Ta_2NiN_{2.5}$ have small ranges. Their crystal structures are derived from that of TaN. Metal atoms are arranged hexagonally with the layer sequence ABACABAC. The ordered distribution of metal atoms explains the occurrence of superstructures. Whereas the elementary cell of Ta_3MnN_4 contains four metal atoms, the arrangement in the $Ta_2MeN_{2.5}$ compounds is such that there are 12 metal atoms in the elementary cell. δ-Tantalum nitride, $TaN_{0.8-0.9}$, also forms with manganese a further hexagonal ternary phase. Nitrogen is octahedrally coordinated in all these double nitrides. They are prepared when a metal alloy of the corresponding composition is melted at 1500°C in a high-frequency induction furnace and then nitrided in a stream of ammonia at 650°–950°C (*157*).

Quite irregular structures occur for $Ti_{0.7}Co_{0.3}N$, $Ti_{0.7}Ni_{0.3}N$, $Mo_{0.8}Co_{0.8}N_{0.9}$, and $Mo_{0.8}Ni_{0.8}N_{0.9}$. These nitrides, which crystallize in the hexagonal system, have the tungsten carbide lattice. The metal atoms are

in a simple hexagonal arrangement and the structure has been related to that of nickel arsenide (*156*).

It will be impossible here to deal with the numerous ternary nitrides that have been isolated from special steels, although some carbidenitrides which occur in steels will be discussed (Section III,A,2). The effect of nitrogen on steel has been the subject of much research in, for example, the cases of chromium-, chromium/nickel-, and chromium/manganese-steels, and steels both with and without a substantial carbon content have been considered (*113*).

c. Mixed Crystals of the Perovskite Type. Mixed crystals of the composition $Mn_{4-x}Me_xN_{1-x/4}\square_{x/4}$ (where Me = Cr, Mn, Ni, Cu, or Zn, and $\square$ denotes holes in the nitrogen sublattice), derived from Mn_4N, the ϵ-phase in the system Mn/N, have been investigated. Incorporation of Me depends on the stability of the binary nitrides of the competing metals. Chromium substitutes manganese in the middle of the face of the unit cell to form a nitrogen-chromium bond. The incorporation of manganese is reflected in the breadth of the Mn_4N phase (cf. Section II,A,2,e). Nickel, copper, and zinc are incorporated in the 000 sites, which does not allow nitrogen-metal bonds to be formed. In addition, nitrogen is substituted by carbon. Lattice constants decrease with incorporation of Cr and Mn (cf. Fig. 15) and rise with that of Ni, Cu, and Zn. Like Mn_4N, the mixed crystals are ferrimagnetic. Curie points rise somewhat as the Mn, Cr, and C content is increased and fall as a result of the incorporation of Cu, Zn, and Ni. Magnetic moments per unit cell depend systematically on the foreign metal content, as may be seen from Fig. 15 (*80, 86*).

Detailed conclusions about spin distribution among separate atom sites cannot be drawn on the basis of saturation measurements. But the systematic changes in saturation magnetism may be explained as follows: the moment of Mn_4N may, on the basis of neutron diffraction studies, be formulated as the difference of two sublattices (*167*):

$$1.14\mu_B = \underset{Mn_c}{(3.84} - 3 \times \underset{Mn_f}{0.90})\mu_B$$

Substitution of nitrogen by carbon involves the withdrawal of one electron per atom of nonmetal (*13, 168*). A hole at a nitrogen site leads to a loss of three electrons, and replacement of Mn_f by Cr results in a further loss of one electron, in addition to the effect associated with the nitrogen hole. Reduction in the electron concentration in the Mn_f lattice leads to increase of the Mn_f moment with spin decoupling and a lowering of the resulting total moment of the unit cell.

Nickel, copper, and zinc may be substituted for Mn_c. These metals give an increase in the electron concentration in the Mn_c lattice with spin

pairing and also produce a decrease in the total moment by creating nitrogen vacancies. The overall result is a lowering of both the Mn_c moment and the total moment of the unit cell (*86*).

Neutron diffraction studies of two specimens with vacancies in the nitrogen sublattice are in agreement with this concept as far as the total moment is concerned, but they cast doubt on the interpretation suggested (*168*). Results with the mixed crystals $Mn_{4-x}In_xN$ and $Mn_{4-x}Sn_xN$ (*114*) are not in good agreement with those above. There are, however, special considerations which explain the discrepancy: these mixed crystals have no vacancies in the nitrogen sublattice, the substituting atoms are very much

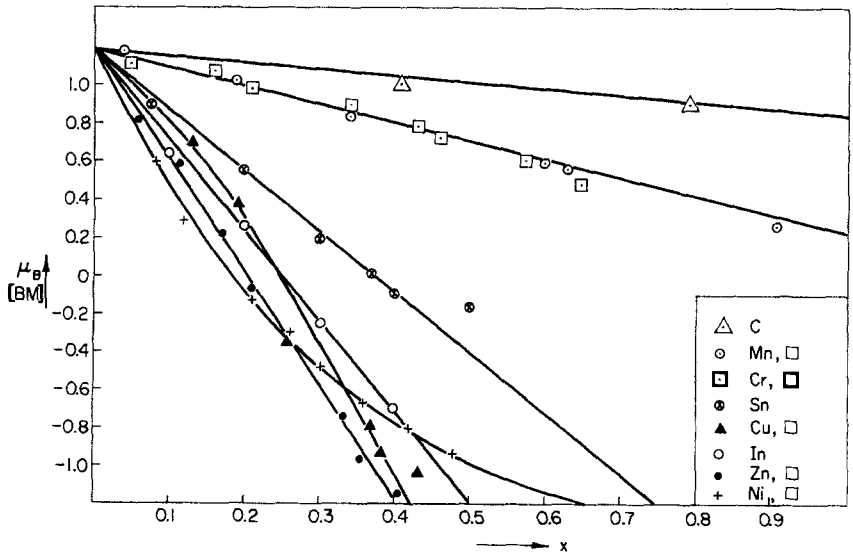

FIG. 15. Magnetic moments of the mixed crystals $Mn_{4-x}Me_xN_{1-x/4}\square_{x/4}$ and $Mn_4N_{1-x/4}C_{x/4}$ (*80, 86*), $Mn_{4-x}In_xN$ and $Mn_{4-x}Sn_xN$ (*114*).

larger, and the number of electrons transferred to a band for Group 3b and 4b elements is certainly not proportional to the group number.

Ternary ferromagnetic compounds may be derived from Fe_4N in which iron in the 000 position is replaced by nickel or platinum. These were prepared by Wiener and Berger with the object of elucidating the magnetic structure of Fe_4N (*176*). Mixed crystals of the type $Fe_{4-x}Ni_xN$ with $0 \leq x \leq 3$ were subject to detailed magnetic investigation over the whole composition range (*45*). The Curie point of $NiFe_3N$ is at 487°C and that of Fe_3PtN at 369°C (*176*). From the saturation magnetization the magnetic moment per unit formula was found to be 7.2 μ_B for Fe_3NiN and 7.76 μ_B for Fe_3PtN. The three iron atoms at the face centers retain their magnetic

moments of 2 μ_B per Fe and, for nickel and platinum in 000, 1 μ_B is to be expected, leading to a total of 7 μ_B per unit formula for both compounds. The differences of +0.2 μ_B and 0.76 μ_B between the measured magnetic moments and those to be expected from the model are to be associated with the contributions from the s-bands of the crystals (*44*).

Further nickel may be substituted for iron in the face centers (*5*); these nickel atoms have a moment of 0 μ_B because the metal-nitrogen bond is covalent (*44*). When yet more nitrogen is incorporated, the tetragonal compound FeNiN is formed. This no longer has the perovskite structure, although structurally it is directly related to $Fe_{4-x}Ni_xN$ (*5*, *171*). This additional nitrogen increases the concentration of electrons so much that ferromagnetic coupling disappears and FeNiN is paramagnetic (*45*).

d. T/M Phases. A group of double nitrides has been discovered recently whose structures are determined by the coexistence of a transition metal (T) and a b-group element (M). The symbols T and M will be used in this section in place of Me. The phases may be derived from those of binary transition metal nitrides that have been discussed so far as follows: nitrogen in the T/M phases is again surrounded by six transition metal atoms in what is essentially an octahedral arrangement, and the b-group atom is not bonded to nitrogen (*64*).

"Perovskite phases," T_3MN: The perovskite phases T_3MN and mixed crystals of the perovskite type (discussed in Section III,A,1,*c*) have much in common. Indeed, from the point of view of crystallography the two sections belong together, but are discussed here from the point of view of chemistry. Table III sets out the T_3MN phases prepared by Stadelmeier which are of interest here (*162–164*). The b-group metal belongs to Groups 1–4. The phases appear to occur preferentially for the elements from manganese to nickel. Compounds with the same structure, however, have been prepared with transition elements of lower atomic number. Thus reaction

TABLE III

T/M PHASES OF THE PEROVSKITE TYPE[a]

Ib		Mn_3CuN[b]			
		Mn_3AgN[b]			
IIb			Fe_3MgN		
		Mn_3ZnN	Fe_3ZnN	Co_3ZnN	Ni_3ZnN
IIIb			Fe_3AlN		Ni_3AlN
	Cr_3GaN[b]	Mn_3GaN[b]	Fe_3GaN	Co_3GaN	
		Mn_3InN	Fe_3InN	Co_3InN	Ni_3InN
IVb			Fe_3GeN	Co_3GeN	
			Fe_3SnN	Co_3SnN	

[a] From Stadelmaier (*162*, *163*); [b] Samson *et al.* (*144*).

of GaN with chromium gives Cr_3GaN (*144*), and Ti_3InN and Ti_3TlN have been prepared from titanium (*76*).

Most of the investigations leave open the question of the extent to which the nitrogen sublattice is occupied (*144, 163*). In the extreme case, when there is no nitrogen in the compound, the perovskite phase goes over to the ordered Cu_3Au phase, in which Au occupies the corners of the cubes. One can, in fact, speak of the perovskite phase as a Cu_3Au phase that is stabilized by nitrogen.

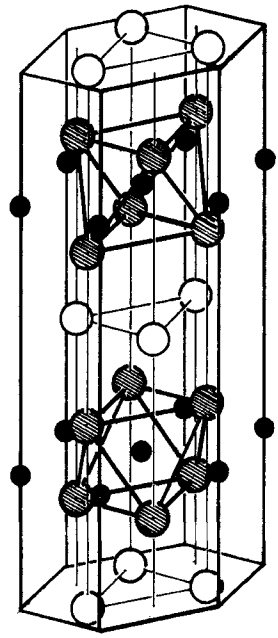

FIG. 16. Lattice of "H phases," T_2MN: ○ M; ◍ T; • N.

"H phases," T_2MN: A further group of ternary phases found by Nowotny has the composition T_2MN. These are designated as "H phases" because they are hexagonal. Compounds of this sort in the first transition series are

Ti_2AlN (*74*)
Ti_2GaN (*75*), V_2GaN (*73*), V_2GeN (*73*)
Ti_2InN (*75*)

These are isotypic with Cr_2AlC and Ti_2SC (*101*). Their structures (cf. Fig. 16) are reminiscent of hexagonal close-packed crystalline intercalated structures, such as Fe_3N, from which they may be derived. Nitrogen atoms are present in the octahedral holes between two transition metal layers that

are perpendicular to the *c*-axis of the hexagonal elementary cell. Above and below these TNT layers there is a layer of atoms of the b-group metal M. The metal atoms are approximately in a hexagonal close-packed arrangement (with the layers A and B) so that in the direction of the *c*-axis there is the sequence $M_AT_BNT_AM_BT_ANT_BM_A$. Incidence of H phases is restricted to transition metals of Groups 4 and 5, but the nature of the b-group element may vary greatly. If it belongs to 2b or 3b, the structure has a high *c/a* ratio and is near to hexagonal close packing. The compound is also predominantly metallic in character. When the b-group element belongs to Group 4 (germanium) or even Group 6 (sulfur, although this is found only in carbides) the axial ratio is smaller and metallic character is less pronounced (*129*).

"β-Manganese phases," T_3M_2X: β-Manganese crystallizes in the cubic system with eightfold and twelvefold position. Double nitrides are derived from this elementary cell. $Mo_{13}Fe_7N_4$, which approximates to $Mo_{12}Fe_8N_4$ or Mo_3Fe_2N, was found (*35*). It has recently been discovered that corresponding compounds may be prepared (V_3Zn_2N and V_3Ga_2N) (*73*) which contain a b-group metal instead of a transition metal at the eightfold position. The number of compounds of this type so far prepared is not large.

"η_2-Carbide phases," T_4M_2N: Ternary nitrides may also be derived from the $E9_3$ type of structure (W_3Fe_3C) or, more precisely, from the "η_2-carbide type" (Mo_4Fe_2C) (*95*). The compound Ti_4Zn_2N may be cited (*73*). In this, transition metal atoms are partly replaced by a b-group atom (Zn). Corresponding oxygen compounds have, for example, the composition Ti_4Cu_2O. In the η_2-carbide phases the nonmetal is in the center of a deformed octahedron.

In all T/M phases formed from a transition metal and a b-group metal that have been described above, it is clear that the metal atom lattice has been stabilized by partially filling the octahedral holes formed by the transition metal atoms.

2. Carbidenitrides

Wöhler (*177*) described a golden yellow lustrous material that he called *Hochofenwürfel*, containing 0.2 of C and 0.8 of N to 1 of Ti. This has since been repeatedly studied, and was shown by X-ray methods to consist of mixed crystals. A continuous series of mixed crystals Ti(N,C) is indeed formed by heating together TiN and TiC to 2400°C. Isotypic nitrides and carbides form such continuous series in many combinations, one proviso being that the radii of the metal atoms shall differ by less than 15%. The same is often true when the metal and nonmetal are varied simultaneously, as in the following combinations: TiN with HfC, VC, NbC; VN with TiC, NbC. Lattice constants of the mixed crystals follow Vegard's rule with

minor deviations (*27*). The carbidenitride systems of Group 4 and 5 transition metals are also interesting technically because, in part accidentally, materials prepared for cermets often contain carbon and nitrogen together.

A detailed phase study of the ternary system in the metal-rich range has been made for *titanium* (*166*). Systematic investigations of electrical properties in TiN/TiC alloys show conductivity to depend mainly on the 4*s* electrons of titanium and to some extent on holes of the 3*d* band. Defect conductivity becomes more pronounced in going from TiN to TiC (*108*). There is a marked minimum in the conductivity for the composition $TiN_{0.75}C_{0.25}$, as is required by the Bilz band scheme in connection with the low density of states at the Fermi boundary of about 8.5 electrons (cf. Section II,D,2). The charge carrier concentration in TiC/TiN mixed crystals, determined by the Hall effect (referred to in Section III,A,1,a), may be interpreted in the same way (*66*).

Systematic study of the *vanadium* carbide nitride system VN/VC/V shows a broad one-phase region for V(N,C), which crystallizes with the NaCl lattice and extends to about $V(N,C)_{0.72}$. In addition, a broad area corresponding to hexagonal close-packed $V_2(N,C)$ joins the two binary phases V_2N and V_2C without gaps (*16*). Specimens were obtained from vanadium powder and carbon by repeated grinding, followed by pressing, heating to 1400°–2000°C, and finally nitriding with nitrogen at 1250°C.

Carbidenitrides of chromium with the NaCl lattice may be obtained from nitrided steels. They are usually isolated by an electrolytic method in which the alloy containing nitride is made the anode (*62*). Since an isotypic chromium carbide does not exist, only part of the nitrogen can be replaced by carbon.

Replacement of nitrogen by carbon in *ε-manganese* nitride, Mn_4N, may be effected up to the composition $Mn_4N_{0.2}C_{0.8}$ by solid-state reaction of the mixture of binary compounds. Saturation magnetization of the mixed crystals, which, like Mn_4N, are ferrimagnetic, falls linearly in accordance with the assumed spin distribution and the decrease in number of valency electrons when nitrogen is replaced by carbon. This decrease leads to an increase in the magnetic moment of the negatively charged sublattice of manganese atoms at face centers, and thus to a lowering of the resultant moment (*13*, *86*) (cf. Fig. 12).

Carbidenitrides of *iron* have been very fully studied and have an important bearing on the properties of special steels. Because of their low thermal stability they cannot be prepared by starting from the two binary compounds. Either the corresponding nitride, made by nitriding with ammonia, is carbided with carbon monoxide, or an iron carbide is nitrided by heating in ammonia (*68*).

As may be seen from the studies of Jack, the results of which are represented in Fig. 17, the composition and structure of carbidenitrides are

directly related to what has been said about the binary nitrides of iron. Orthorhombic nonmetal-rich ζ-carbidenitride extends from Fe_2N to $Fe_2C_{0.75}N_{0.25}$ (*68*). Unlike ζ-Fe_2N, this iron carbidenitride is ferromagnetic. Its Curie point increases with the carbon content and lies between 288° and 350°C (*17*).

The hexagonal carbidenitride, which corresponds to the ϵ-phase in the iron/nitrogen system, has a phase range from $Fe_3(C,N)$ to $Fe_2(C,N)$ and contains a maximum of 16 atom% of C (*68*). It is also ferromagnetic with Curie points in the range −90° to 388°C, depending on the composition (*17*).

In the γ'-phase, Fe_4N, very little nitrogen can be replaced by carbon (*17*, *68*). The carbon-containing Fe_4N phase is also ferromagnetic with a

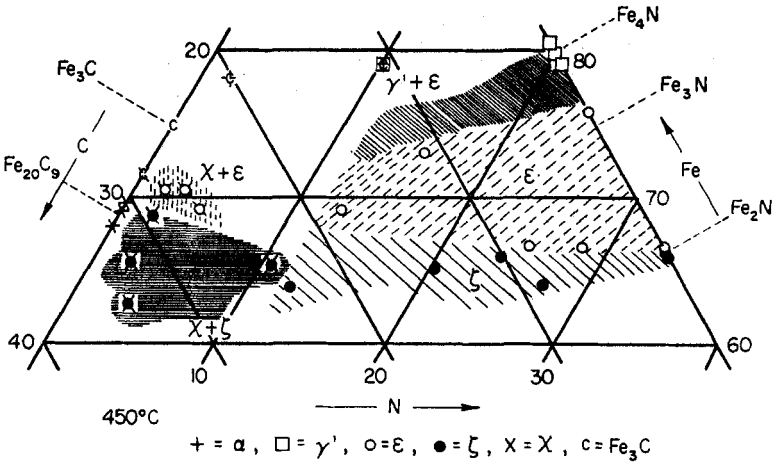

FIG. 17. The iron/carbon/nitrogen system (*68*).

Curie point between 471° and 490°C, depending on the N/C ratio (*17*). It is found by thermomagnetic methods that the γ' type of carbidenitride loses carbon on heating to form hexagonal $Fe_3(C,N)$, which has a high carbon content. There also appears α-Fe containing a little N and C.

Knowledge of iron carbidenitrides is of interest *inter alia* because they enter into the carbonitriding of steels. These processes use baths containing fused alkali cyanides or, in the case of gas cementation, mixtures of nitriding and carbiding gases. In carbonitriding it is thought that the quick-acting nitrogen accelerates subsequent carbiding. This is important because every effort is made to carry through the process at as low a temperature as possible and to do the subsequent hardening operation by relatively mild quenching, e.g., in air or a stream of gas.

Carbidenitrides of *cobalt* are closely comparable with those of iron. The phase richest in nitrogen in the system Co/N is Co_2N, which, like Co_2C, crystallizes in the orthorhombic system. The lattice constants of the two compounds differ little. As a result it is possible when carbiding Co_2N with CO at 340°C gradually to replace all of the nitrogen by carbon. Lattice constants for mixed crystals of $Co_2(N,C)$ change uniformly with the N/C ratio. There is no isotypic carbide Co_3C corresponding to hexagonal Co_3N. As a result, only partial replacement of N by C in Co_3N can be achieved (*25*).

Nickel nitride, Ni_3N, may also be carbided (*69*): both Ni_3N and Ni_3C crystallize in the hexagonal system and their lattice dimensions are almost the same.

3. *Nitride Oxides*

Little is known about nitrides of the first transition series containing oxygen as a second nonmetal. TiN and TiO differ in lattice constants by only about 2% and would therefore be expected to form series of mixed crystals. X-ray studies show, however, that Ti(N,O) specimens, prepared from the binary compounds by sintering at 1700°C, exhibit the unchanged lattice constant of TiN from TiN to $TiN_{0.6}O_{0.4}$. A decrease in the lattice constant to that of TiO follows, indicating a limited solubility of TiN in TiO, but not of TiO in TiN. Pyknometric density determinations, which can give information on the number of vacancies in the cation lattice, provide no further clarification (*155*).

The influence of oxygen on the electrical properties of TiN has been investigated up to about $TiN_{0.5}O_{0.5}$. The specific resistance passes through a minimum at about 40 mole % TiO, while the differential thermoelectric power and Hall coefficient have a minimum at about 20%. The temperature dependence of the specific resistance was also examined: it is first strongly positive and from above about 1200°C strongly negative (*150*). These resistance measurements are not, however, reconcilable with experiments on thin TiN films with a small oxygen content, which were found to be semiconducting (*117*). Further results on nitride oxides are available for vanadium (*140*), chromium (*141*), and cobalt (*89*). Compounds of the metals in question were first nitrided and then oxidized, or vice versa. The products were believed to contain nitride oxides in addition to oxides and nitrides. These nitride oxides could not, however, be made in an equilibrium reaction.

B. Polar Ternary Compounds

Brief reference may be made to ternary compounds containing, in addition to a transition metal and nitrogen, another base metal (lithium) or a very electronegative nonmetal (a halogen). The nature of such ternary

compounds is determined largely by the tendency of these elements to go over to the ionic state.

1. Polar Double Nitrides

When lithium nitride is heated in a nitrogen atmosphere with finely divided cobalt, nickel, or copper, the metal enters the Li_3N lattice and is simultaneously nitrided to an oxidation state of +1. While Co_3N, Ni_3N, and Cu_3N cannot be obtained from the metal and nitrogen (Section II,C,1), nitrogen uptake occurs during the process of incorporation in lithium nitride. The heavy metal atom is taken up on $00\frac{1}{2}$ sites in hexagonal Li_3N up to a composition of about $Li_{2.5}Me_{0.5}N$. The mixed crystals retain the predominantly saltlike character of Li_3N (*143*).

Corresponding reactions of Li_3N with titanium, vanadium, chromium, manganese, and iron, or reaction with the binary nitrides of these metals, lead in a nitrogen atmosphere to compounds in which one finds oxidation states of the metal with respect to nitrogen which do not occur in the binary nitrides: e.g., Li_5TiN_3 (*91*), Li_7VN_4 (*81*), Li_9CrN_5 (*84*), Li_7MnN_4 (*79*), Li_3FeN_2 (*38*). Whereas the limiting composition in the binary nitrides of titanium, vanadium, and chromium is MeN, these three metals here occur in their highest oxidation states. This is, however, not so for manganese and iron, although oxidation states of five or three with respect to nitrogen are stabilized. The electrovalent composition, high melting points, and ready hydrolysis of the compounds indicate that they have predominantly polar structures.

In these ternary nitrides no complex ions occur in spite of the high charge on the transition metal. This is because of the high charge on the Ni^{3-} ion. The compounds from titanium to manganese crystallize with a superstructure of the antifluorite lattice. The equivalent lattice positions are known for Li_5TiN_3, Li_7VN_4, and Li_7MnN_4. In all cases nitrogen ions are cubically close packed; metal ions are in the tetrahedral holes and, unlike nitrogen atoms in intercalation compounds, the nitrogen ions are surrounded by eight cations. There are always two cations per anion. The "AB_2 character" of the compounds is emphasized by the fact that mixed crystals are formed with Li_2O, which also crystallizes with an antifluorite lattice (*91*).

2. Nitride Halides

The nitride halides TiNCl, TiNBr, and TiNI may be obtained by ammonolysis of the halides at elevated temperatures. These titanium compounds decompose at high temperatures and hydrolyze very readily. The corresponding compounds of the heavier metals zirconium and especially thorium are much more stable thermally and chemically.

The titanium compounds mentioned crystallize isotypically with FeOCl and thus have a pronounced layer lattice. In the rhombic elementary cell the sequence HalTiNNTiHal occurs in the direction of the *c*-axis. Lattice dimensions within the layers are determined by the two close-packed layers of large halogen ions. Thus it happens that both close-packed nitrogen layers are pushed together into a doubly occupied corrugated layer. It may be assumed that the halogens are present as ions. Within the cationic layer $(TiNNTi)_n^{2n+}$ the polar component of the bond should, however, be small (*85*).

ACKNOWLEDGMENT

I thank Dr. H. Seidel and Dipl.-Chem. H. Jacobs for their enthusiastic help in preparing this article.

REFERENCES

1. Agte, C., and Moers, K., *Z. Anorg. Allgem. Chem.* **198,** 233 (1931).
2. Akishin, P. A., and Klodeev, Y. S., *Zh. Neorgan. Khim.* **7,** 941 (1962).
3. Akishin, P. A., and Klodeev, Y. S., *Russ. J. Inorg. Chem.* (*English Transl.*) **7,** 486 (1962).
4. Amaya, K., Ajiro, Y., Yasuoka, H., Abe, H., Matsuura, M., and Hirai, A., *J. Phys. Soc. Japan* **19,** 413 (1964).
5. Arnott, R. J., and Wold, A., *Phys. Chem. Solids* **15,** 152 (1960).
6. Baratashivili, J. B., Fedotov, V. P., Samarin, A. M., and Berethiani, J. B., *Fiz. Khim. Osnovy Proizv. Stali, Akad. Nauk SSSR, Inst. Met. Tr. 6-oi Eshestoi J. Konf., Moscow* p. 294 (1961).
7. Becker, K., *Z. Physik* **34,** 185 (1933).
8. Becker, K., and Ebert, F., *Z. Physik* **31,** 268 (1925).
9. Bernier, R., *Ann. Chim.* (*Paris*) [12] **6,** 104 (1951).
10. Bilz, H., *Z. Physik* **153,** 338 (1958).
11. Blix, R., *Z. Physik. Chem.* **B3,** 229 (1929).
12. Blum, A., *Planseeber. Pulvermet.* **10,** 72 (1962).
13. Bouchaud, J. P., and Fruchart, R., *Bull. Soc. Chim. France* No. 2, 1579 (1964).
14. Brager, A., *Acta Physicochim. URSS* **11,** 617 (1939).
15. Brauer, G., and Schnell, W. D., *J. Less-Common Metals* **6,** 326 (1964).
16. Brauer, G., and Schnell, W. D., *J. Less-Common Metals* **7,** 23 (1964).
17. Bridelle, R., *Ann. Chim.* (*Paris*) [12] **10,** 824 (1955).
18. Brisi, C., *Met. Ital.* **47,** 405 (1955).
19. Brisi, C., and Abbattista, F., *Ric. Sci.* **29,** 1402 (1959).
20. Burdese, A., *Met. Ital.* **47,** 357 (1955).
21. Burdese, A., *Met. Ital.* **49,** 195 (1957).
22. Burdese, A., *Met. Ital.* **50,** 529 (1958).
23. Burdese, A., and Abbattista, F., *Atti Accad. Sci. Torino, Classe Sci. Fis. Mat. Nat.* **93,** 340 (1958–1959).
24. Campbell, I. E., Powell, C. F., Nowicki, D. H., and Gonser, B. W., *J. Electrochem. Soc.* **96,** 318 (1949).
25. Clarke, J., and Jack, K. H., *Chem. Ind.* (*London*) p. 1004 (1951).
26. Corliss, L. M., Elliott, N., and Hastings, J. M., *Phys. Rev.* **117,** 929 (1960).
27. Duwez, P., and Odell, F., *J. Electrochem. Soc.* **97,** 299 (1950).

28. Ehrlich, P., *Z. Anorg. Chem.* **259,** 1 (1949).
29. Eisenhut, O., and Kaupp, E., *Z. Elektrochem.* **36,** 392 (1930).
30. Elliott, N., *Phys. Rev.* **129,** 1120 (1963).
31. Emmett, P. H., Hendricks, S. B., and Brunauer, S., *J. Am. Chem. Soc.* **52,** 1456 (1930).
32. Epelbaum, V., and Brager, A., *Acta Physicochim. URSS* **13,** 595 (1940).
33. Epelbaum, V., and Ormont, B., *Acta Physicochim. URSS* **22,** 319 (1947).
34. Eriksson, S., *Jernkontorets Ann.* **118,** 530 (1934).
34a. Ern, V., and Switendick, A. C., *Phys. Rev.* **137,** A1927 (1965).
35. Evans, D. A., and Jack, K. H., *Acta Cryst.* **10,** 769 (1957).
36. Fast, J. D., *Philips Tech. Rev.* **10,** 27 (1948).
37. Foster, L. S., AECD 2942 (1945).
38. Frankenburger, W., Andrussow, L., and Dürr, F., *Z. Elektrochem.* **34,** 632 (1928).
39. Frazer, B. C., *Phys. Rev.* **112,** 751 (1958).
40. Friederich, E., and Sittig, L., *Z. Anorg. Allgem. Chem.* **143,** 293 (1925).
41. Fry, A., *J. Iron Steel Inst. (London)* **125,** 191 (1932).
42. Goodenough, J. B., *Phys. Rev.* **117,** 1442 (1960).
43. Goodenough, J. B., *Phys. Rev.* **120,** 67 (1960).
44. Goodenough, J. B., "Magnetism and the Chemical Bond." Wiley (Interscience), New York, 1963.
45. Goodenough, J. B., Wold, A., and Arnott, R. J., *J. Appl. Phys.* **31,** Suppl., 342 (1960).
46. Guillaud, C., and Creveaux, H., *Compt. Rend.* **222,** 1170 (1946).
47. Guillaud, C., and Wyart, J., *J. Rech. Centre Natl. Rech. Sci. Lab. Bellevue (Paris)* **3,** 123 (1947).
48. Hägg, G., *Nova Acta Regiae Soc. Sci. Upsaliensis* [4] **7,** No. 1, 95 (1929).
49. Hägg, G., *Z. Physik. Chem.* **B4,** 346 (1929).
50. Hägg, G., *Z. Physik. Chem.* **B6,** 229 (1929).
51. Hägg, G., *Z. Physik. Chem.* **B12,** 33 (1931).
52. Hägg, G., *IVA* **24,** 345 (1953).
53. Hahn, H., *Z. Anorg. Chem.* **258,** 58 (1949).
54. Hahn, H., and Konrad, A., *Z. Anorg. Allgem. Chem.* **264,** 181 (1951).
55. Hansen, M., "Constitution of Binary Alloys," 2nd ed. McGraw-Hill, New York, 1958.
56. Hardy, G. F., and Hulm, D. K., *Phys. Rev.* **93,** 1004 (1954).
57. Hendricks, S. B., and Kosting, P. K., *Z. Krist., Abt. A Z. Krist. Mineral. Petrog.* **74,** 511 (1930).
58. Hilpert, R. S., Hoffmann, A., and Huch, F. H., *Ber. Deut. Chem. Ges.* **72B,** 848 (1939).
59. Hoch, M., Dingledy, D. P., and Johnston, L., *J. Am. Chem. Soc.* **77,** 304 (1955).
60. Holmberg, B., *Acta Chem. Scand.* **16,** 1255 (1962).
61. Hume-Rothery, W., *Phil. Mag.* [7] **44,** 1154 (1953).
62. Hume-Rothery, W., Raynor, G. V., and Little, A. T., *J. Iron Steel Inst. (London)* **145,** 129 (1942).
63. Humphrey, G. L., *J. Am. Chem. Soc.* **73,** 2261 (1951).
64. Hüttig, G. F., *Kolloid-Z.* **97,** 281 (1941).
65. Imai, Y., and Ishizaki, T., *Sci. Rept. Res. Inst. Tohoku Univ. Ser. A* **14,** 203 (1962).
66. Ito, F., Tsuchida, T., and Takaki, H., *J. Phys. Soc. Japan* **19,** No. 1, 136 (1964).
67. Jack, K. H., *Proc. Roy. Soc.* **A195,** 34 (1948).
68. Jack, K. H., *Proc. Roy. Soc.* **A195,** 41 (1948).
69. Jack, K. H., *Acta Cryt.* **3,** 392 (1950).
70. Jack, K. H., *Proc. Roy. Soc.* **A208,** 200 (1951).

71. Jack, K. H., *Proc. Roy. Soc.* **A208,** 216 (1951).
72. Jack, K. H., *Acta Cryst.* **5,** 404 (1952).
73. Jeitschko, W., Nowotny, H., and Benesovsky, F., *Monatsh. Chem.* **95,** 156 (1964).
74. Jeitschko, W., Nowotny, H., and Benesovsky, F., *Monatsh. Chem.* **94,** 1198 (1963).
75. Jeitschko, W., Nowotny, H., and Benesovsky, F., *Monatsh. Chem.* **95,** 178 (1964).
76. Jeitschko, W., Nowotny, H., and Benesovsky, F., *Monatsh. Chem.* **95,** 436 (1964).
77. Janeff, W., *Z. Physik* **142,** 619 (1955).
78. Joyner, T. B., and Verhoek, F. H., *J. Am. Chem. Soc.* **83,** 1070 (1961).
79. Juza, R., Anschütz, E., and Puff, H., *Angew. Chem.* **71,** 161 (1959).
80. Juza, R., Deneke, K., and Puff, H., *Z. Elektrochem.* **63,** 551 (1959).
81. Juza, R., Gieren, W., and Haug, J., *Z. Anorg. Allgem. Chem.* **300,** 61 (1959).
82. Juza, R., and Hahn, H., *Z. Anorg. Allgem. Chem.* **239,** 282 (1938).
83. Juza, R., and Hahn, H., *Z. Anorg. Allgem. Chem.* **241,** 172 (1939).
84. Juza, R., and Haug, J., *Z. Anorg. Allgem. Chem.* **309,** 276 (1961).
85. Juza, R., and Heners, J., *Z. Anorg. Allgem. Chem.* **332,** 159 (1964).
86. Juza, R., and Puff, H., *Z. Elektrochem.* **61,** 810 (1957).
87. Juza, R., Puff, H., and Wagenknecht, F., *Z. Elektrochem.* **61,** 804 (1957).
88. Juza, R., and Rabenau, A., *Z. Anorg. Allgem. Chem.* **285,** 212 (1956).
89. Juza, R., and Sachsze, W., *Z. Anorg. Chem.* **253,** 95 (1947).
90. Juza, R., and Sachsze, W., *Z. Anorg. Allgem. Chem.* **251,** 201 (1943).
91. Juza, R., Weber, H. H., and Meyer-Simon, E., *Z. Anorg. Allgem. Chem.* **273,** 48 (1953).
92. Kelley, K. K., *U.S. Bur. Mines, Bull.* No. 407, 66 (1937).
93. Kieffer, R., and Benesovsky, F., "Hartstoffe." Springer, Wien, 1963.
94. Kieffer, R., and Schwarzkopf, P., "Hartstoffe und Hartmetalle." Springer, Wien, 1953.
95. Kiessling, R., 1952, *Proc. Intern. Symp. Reactivity Solids, Gothenburg, 1952* p. 1065. Elanders Boktrycheri Actiebolag, Gothenburg, Sweden (1954).
96. Kischkin, S. T., and Panassjuk, J. O., *Dokl. Akad. Nauk SSSR* **113,** 1263 (1957).
97. Klemm, W., and Schüth, W., *Z. Anorg. Allgem. Chem.* **201,** 24 (1931).
98. Kontorowitsch, J. E., and Ssowalow, G. A., *Izv. Akad. Nauk SSSR, Otd. Teckhn. Nauk* p. 1675 (1949).
99. Krebs, H., *Acta Cryst.* **9,** 95 (1956).
100. Krichevskii, I. R., and Khazanova, N. E., *Zh. Fiz. Khim.* **21,** 719 (1947).
101. Kudielka, H., and Rohde, H., *Z. Krist.* **114,** 447 (1960).
102. Kume, K., and Yamagishi, H., *J. Phys. Soc. Japan* **19,** 414 (1964).
103. Kuriyama, M., Hosoya, S., and Suzuki, T., *Phys. Rev.* **130,** 898 (1963).
104. Landolt, H., and Börnstein, R., "Zahlenwerte und Funktionen aus Physik, Chemie, Astronomie, Geophysik und Technik," 6th ed., Vol. 2, Pt. 4. Springer, Berlin, 1961.
105. Lehrer, E., *Z. Elektrochem.* **36,** 383 (1930).
106. Lehrer, E., *Z. Elektrochem.* **36,** 460 (1930).
107. Lihl, F., Ettmayer, P., and Kutzelnigg, A., *Z. Metallk.* **53,** 715 (1962).
108. L'vov, S. M., Nemchenko, V. F., and Samsonov, G. V., *Ukr. Fiz. Zh.* **7,** 331 (1962).
109. McGee, S. W., and Sump, C. H., *ASTM Bull.* **217,** 58 (1956).
110. Mah, A. D., *J. Am. Chem. Soc.* **80,** 2954 (1958).
111. Mah, A. D., *U.S. Bur. Mines, Rept. Invest.* **5529,** (1960).
112. Mah, A. D., *U.S. Bur. Mines, Rept. Invest.* **6177,** 1–8 (1963).
113. Maratray, F., *Publ. Inst. Rech. Siderurgie (Saint-Germain-en-Laye) Ser. B.* No. 75, 47 (1954).
114. Mekata, M., *J. Phys. Soc. Japan* **17,** 796 (1962).

115. Moers, K., *Z. Anorg. Allgem. Chem.* **198,** 243 (1931).
116. Mott, N. F., *Nuovo Cimento* [10] **7,** Suppl., 312 (1958).
117. Münster, A., *Angew. Chem.* **69,** 281 (1957).
118. Münster, A., and Ruppert, W., *Z. Elektrochem.* **57,** 564 (1953).
119. Münster, A., and Schlamp, C., *Z. Physik. Chem. (Frankfurt)* [N.F.]. **13-15,** 59 and 176 (1957–1958).
120. National Bureau of Standards, Washington 1947–1959, Selected values of chemical thermodynamic properties. *Natl. Bur. Std. (U.S.) Circ.* 500, reprint 1961.
121. Néel, L., *Ann. Phys. (Paris)* [12] **3,** 137 (1948).
122. Nemnonow, S. A., and Menschikow, A. Z., *Izv. Akad. Nauk SSSR, Ser. Fiz.* **23,** 578 (1959).
123. Neshpor, V. S., *in* "Refractory Transition Metal Compounds; High Temperature Cermets" (G. V. Samsonov, ed.), pp. 62–106. Academic Press, New York, 1964 (translated from Russian).
124. Neumann, B., Kröger, C., and Haebler, H., *Z. Anorg. Allgem. Chem.* **196,** 65 (1931).
125. Neumann, B., Kröger, C., and Kunz, H., *Z. Anorg. Allgem. Chem.* **218,** 379 (1934).
126. Nishiyama, Z., and Iwanaga, R., *Mem. Inst. Sci. Ind. Res., Osaka Univ.* **9,** 74 (1952).
127. Nowotny, H., Benesovsky, F., Brukl, C., and Schob, O., *Monatsh. Chem.* **92,** 403 (1961).
128. Nowotny, H., Benesovsky, F., and Rudy, E., *Monatsh. Chem.* **91,** 348 (1960).
129. Nowotny, H., Jeitschko, W., and Benesovsky, F., *Planseeber. Pulvermet.* **12,** 31 (1964).
130. Opfermann, W., *Monatsber. Deut. Akad. Wiss. (Berlin)* **6,** 92 (1964).
131. Palty, A. E., Margolin, H., and Nielsen, J. P., *Trans. Am. Soc. Metals* **46,** 312 (1954).
132. Paranjpe, V. G., Cohen, M., Bever, M. B., and Floe, C. F., *Trans. J. Metals* **188,** 261 (1950).
133. Pauling, L., *J. Am. Chem. Soc.* **69,** 542 (1947).
134. Pauling, L., "The Nature of the Chemical Bond." Cornell Univ. Press, Ithaca, New York, 1960.
135. Pinsker, Z. G., and Abrosimowa, L. N., *Kristallografiya* **3,** 28 (1958).
136. Pinsker, Z. G., and Kaverin, S. V., *Dokl. Akad. Nauk SSSR* **95,** 519 (1954).
137. Pinsker, Z. G., and Kaverin, S. V., *Kristallografiya* **2,** 386 (1957).
138. Ratner, A. W., and Leonowa, L. G., *Teploenergetika* **7,** No. 1, 59 (1960).
139. Robbins, M., and White, J. G., *Phys. Chem. Solids* **25,** 717 (1964).
140. Roubin, M. P., and Pâris, J. M., *Compt. Rend.* **260,** 3088 (1965).
141. Roubin, M. P., and Pâris, J. M., *Compt. Rend.* **260,** 3981 (1965).
142. Rundle, R. E., *Acta Cryst.* **1,** 180 (1948).
143. Sachsze, W., and Juza, R., *Z. Anorg. Chem.* **259,** 278 (1949).
144. Samson, C., Bouchaud, J. P., and Fruchart, R., *Compt. Rend.* **259,** 392 (1964).
145. Samsonov, G. V., *Dokl. Akad. Nauk SSSR* **83,** 689 (1953).
146. Samsonov, G. V. (ed.), *in* "Refractory Transition Metal Compounds; High Temperature Cermets," pp. 1–12. Academic Press, New York, 1964 (translated from Russian).
147. Samsonov, G. V., Kosolapova, T. Y., Lyutana, M. D., and Marenko, G. N., *Redkozem. Elementy, Akad. Nauk SSSR, Inst. Geokhim. i. Analit. Khim.* p. 8 (1963).
148. Samsonov, G. V., and Neshpor, V. S., *Vopr. Poroshkovoi Met i. Prochnosti Materiolov, Akad. Nauk Ukr. SSR* No. 7, 99 (1959).

149. Samsonov, G. V., and Verkhoglyadova, T. S., *Dokl. Akad. Nauk SSSR* **142,** 608 (1962).
150. Samsonov, G. V., Verkhoglyadova, T. S., L'vov, S. M., and Nemschenko, V. F., *Dokl. Akad. Nauk SSSR,* **142,** 862 (1962).
151. Sano, K., *J. Chem. Soc. Japan* **58,** 981 (1937).
152. Satô, S., *Sci. Papers Inst. Phys. Chem. Res. (Tokyo)* **34,** 1356 (1938).
153. Schenk, R., and Kortengräber, A., *Z. Anorg. Allgem. Chem.* **210,** 273 (1933).
154. Schmitz-Dumont, O., *Z. Elektrochem.* **60,** 866 (1956).
155. Schmitz-Dumont, O., and Steinberg, K., *Naturwissenschaften* **41,** 117 (1954).
156. Schönberg, N., *Acta Met.* **2,** 427 (1954).
157. Schönberg, N., *Acta Chem. Scand.* **8,** 213 (1954).
158. Shirane, G., Takei, W. J., and Ruby, S. L., *Phys. Rev.* **126,** 49 (1962).
159. Shomate, C. H., *J. Am. Chem. Soc.* **68,** 310 (1946).
160. Shomate, C. H., and Young, F. E., *J. Am. Chem. Soc.* **66,** 771 (1944).
161. Shull, C. G., Wollan, E. O., and Koehler, W. C., *Phys. Rev.* **84,** 912 (1951).
162. Stadelmaier, H. H., and Fraker, A. C., *Z. Metallk.* **53,** 48 (1962).
163. Stadelmaier, H. H., *Z. Metallk.* **52,** 758 (1961).
164. Stadelmaier, H. H., and Tong, S. Y., *Z. Metallk.* **52,** 477 (1961).
165. Stokes, C. S., and Knipe, W. W., *Ind. Eng. Chem.* **52,** 287 (1960).
166. Stone, L., and Margolin, M., *J. Metals* **5,** 1498 (1953).
167. Takei, W. J., Shirane, G., and Frazer, B. C., *Phys. Rev.* **119,** 122 (1960).
168. Takei, W. J., Heikes, R. R., and Shirane, G., *Phys. Rev.* **125,** 1893 (1962).
169. Terao, N., *Naturwissenschaften* **45,** 620 (1958).
170. Terao, N., *Mem. Sci. Rev. Met.* **57,** 96 (1960).
171. Terao, N., *J. Phys. Soc. Japan* **17,** Suppl. BII, 242 (1962).
171a. van Arkel, A. E., and de Boer, J. H., *Z. Anorg. Allgem. Chem.* **148,** 345 (1925).
172. Wain, H. L., Henderson, F., Johnstone, S. T. M., and Louat, N., *J. Inst. Metals* **86,** Pt. 6, 281 (1958).
173. Watt, G. W., and Davies, D. D., *J. Am. Chem. Soc.* **70,** 3753 (1948).
174. Weaver, C. W., *Nature* **180,** 806 (1957).
175. Westphal, R. C., and Glatter, J., *Mater. Methods* **40,** 100 (1954).
176. Wiener, G. W., and Berger, J. A., *J. Metals* **7,** *AIME Trans.* **203,** 360 (1955).
177. Wöhler, F., *Ann. Chem.* **73,** 34 (1850).
178. Wold, A., Arnott, R. J., and Menyuk, N., *J. Phys. Chem.* **65,** 1068 (1961).
179. Yousef, Y. L., Girgis, R. K., and Mikhail, H., *J. Chem. Phys.* **23,** 959 (1955).
180. Zwicker, U., *Z. Metallk.* **42,** 274 (1951).